Available online at www.sciencedirect.com
ScienceDirect
Biomaterials 28 (2007) 3217–3227
Biomaterials
www.elsevier.com/locate/biomaterials

Injectable biodegradable hydrogel composites for rabbit marrow mesenchymal stem cell and growth factor delivery for cartilage tissue engineering

Hansoo Park[a], Johnna S. Temenoff[b], Yasuhiko Tabata[c], Arnold I. Caplan[d], Antonios G. Mikos[a,*]

[a]*Department of Bioengineering, Rice University, MS-142, P.O. Box 1892, Houston, TX 77251-1892, USA*
[b]*Wallace H. Coulter Department of Biomedical Engineering, Georgia Institute of Technology, 313 Ferst Dr., Atlanta, GA 30332-0535, USA*
[c]*Department of Biomaterials, Field of Tissue Engineering, Institute for Frontier Medical Sciences, Kyoto University, 53 Kawara-cho Shogoin, Sakyo-ku, Kyoto 606-8507, Japan*
[d]*Skeletal Research Center, Department of Biology, Case Western Reserve University, Cleveland, OH, USA*

Received 31 January 2007; accepted 27 March 2007
Available online 5 April 2007

Abstract

We investigated the development of an injectable, biodegradable hydrogel composite of oligo(poly(ethylene glycol) fumarate) (OPF) with encapsulated rabbit marrow mesenchymal stem cells (MSCs) and gelatin microparticles (MPs) loaded with transforming growth factor-β1 (TGF-β1) for cartilage tissue engineering applications. Rabbit MSCs and TGF-β1-loaded MPs were mixed with OPF, a poly(ethylene glycol)-diacrylate crosslinker and the radical initiators ammonium persulfate and *N,N,N′,N′*-tetramethylethylenediamine, and then crosslinked at 37 °C for 8 min to form hydrogel composites. Three studies were conducted over 14 days in order to examine the effects of: (1) the composite formulation, (2) the MSC seeding density, and (3) the TGF-β1 concentration on the chondrogenic differentiation of encapsulated rabbit MSCs. Bioassay results showed no significant difference in DNA amount between groups, however, groups with MPs had a significant increase in glycosaminoglycan content per DNA starting at day 7 as compared to controls at day 0. Chondrocyte-specific gene expression of type II collagen and aggrecan were only evident in groups containing TGF-β1-loaded MPs and varied with TGF-β1 concentration in a dose-dependent manner. Specifically, type II collagen gene expression exhibited a 161 ± 49-fold increase and aggrecan gene expression a 221 ± 151-fold increase after 14 days with the highest dose of TGF-β1 (16 ng/ml). These results indicate that encapsulated rabbit MSCs remained viable over the culture period and differentiated into chondrocyte-like cells, thus suggesting the potential of OPF composite hydrogels as part of a novel strategy for localized delivery of stem cells and bioactive molecules.

Keywords: Cartilage tissue engineering; Marrow mesenchymal stem cells; Gelatin microparticles; Injectable hydrogels; Tgf-β1

1. Introduction

Current treatments for cartilage lesions, including autografts and subchondral drilling, have significant complications such as secondary site morbidity and incomplete defect healing [1]. Over the past decade, tissue engineering approaches have been developed, which combine cells, bioactive molecules and scaffolding materials [2]. Particularly, during this time, synthetic, biodegradable hydrogels have been designed as cell and growth factor delivery systems in orthopedic tissue engineering. These materials can provide support during the healing process and are often used in an injectable form as a minimally invasive method to fill irregularly shaped defects [3–5].

Recently, a novel class of injectable hydrogels based on the oligomer oligo(poly(ethylene glycol) fumarate) (OPF) has been developed for the delivery of cells and growth factors to cartilage lesions [6–9]. The poly(ethylene glycol) (PEG) repeating unit imparts water solubility to this

*Corresponding author. Tel.: +1 713 348 5355.
E-mail address: mikos@rice.edu (A.G. Mikos).

0142-9612/$ - see front matter © 2007 Elsevier Ltd. All rights reserved.
doi:10.1016/j.biomaterials.2007.03.030

oligomer, while its repeating double bonds facilitate crosslinking to form a three-dimensional gel structure. Biodegradation of OPF hydrogels is possible through the hydrolysis of the ester linkages in the fumarate group [10,11]. Additionally, peptide sequences can be incorporated before OPF crosslinking to promote specific, interactions with cells [12,13]. Thus, as an injectable, *in situ* crosslinkable, and biodegradable oligomer, OPF is a suitable candidate for minimally invasive, localized cell and drug delivery therapies.

In a previous study, it was demonstrated that rat marrow mesenchymal stem cells (MSCs) could be encapsulated in OPF and their differentiation induced over 28 days *in vitro* with the addition of osteogenic supplements to the culture medium [14,15]. In another series of experiments, our laboratory has demonstrated that incorporating gelatin microparticles (MPs) into OPF hydrogel scaffolds is a useable strategy for localized and sustained release of a growth factor [9]. Specifically, gelatin MPs loaded with transforming growth factor-β1 (TGF-β1) were encapsulated into OPF hydrogels and the rate of TGF-β1 release could be controlled by altering OPF formulation and the crosslinking extent of gelatin MPs [9]. Building on these studies, TGF-β1-loaded gelatin microspheres were then embedded with bovine chondrocytes in OPF hydrogels. The results demonstrated that the presence of loaded gelatin MPs promoted cell proliferation while maintaining a chondrocytic phenotype [7].

The findings from these *in vitro* as well as *in vivo* studies suggest that OPF hydrogel composites possess distinct advantages for use *in vivo* [6]. In addition to holding cells at the defect site, the localized, sustained growth factor release should encourage cell proliferation, differentiation and matrix production in the hydrogel while preventing bolus release of TGF-β1, a known pro-inflammatory agent [16], into the joint space. However, recognizing the limited amount of donor tissue for autologous chondrocyte transplantation, we have chosen to focus our attention in the current study on the effects of this carrier system on chondrogenic differentiation of MSCs. Because of the availability of MSCs and the potential for expansion of these cells without affecting their differentiation capacity, this cell source could serve as a key component of future approaches using this hydrogel system to regenerate cartilage lesions.

Thus, the objectives of the present study were to examine the effects of the presence of gelatin microspheres on cell proliferation, gene expression, and matrix production by rabbit MSCs embedded in OPF hydrogels and to determine if chondrogenic differentiation of embedded MSCs could be directed by controlled release of low levels of TGF-β1. An additional objective was to investigate how the proliferation, gene expression and matrix production from encapsulated rabbit MSCs were affected by changes in the local hydrogel environment brought about by alterations in cell seeding density and dose of TGF-β1 released.

2. Materials and methods

2.1. OPF synthesis and characterization

OPF was synthesized from fumaryl chloride and PEG of number average molecular weight 10 kDa according to a previously established method [11]. Oligomer molecular weight ($n = 3$) was determined by gel permeation chromatography (GPC; Model 410; Waters, Milford, PA) using a refractive index detector. Purified OPF was stored at −20 °C and sterilized prior to use by exposure to ethylene oxide for 16 h.

2.2. Gelatin microparticle preparation

Gelatin MPs were fabricated from acidic gelatin (Nitta Gelatin Inc., Osaka, Japan), following established procedures [7]. Briefly, a gelatin solution was prepared by dissolving 5 g gelatin in 45 ml distilled, deionized water (ddH_2O) at 60 °C. Then, this solution was added dropwise to 250 ml chilled olive oil while stirring at 500 rpm. After 30 min, 100 ml chilled acetone (4 °C) was added to the emulsion. After an additional 60 min, the microspheres were collected by filtration and washed with acetone. These MPs were then crosslinked in 0.1 wt% Tween 80 (Sigma, St. Louis, MO) solution with 10 mM glutaraldehyde (GA) (Sigma, St. Louis, MO) while stirring at 500 rpm at 15 °C. After 15 h, crosslinked MPs were collected by filtration, washed with ddH_2O, and then agitated in 25 mM glycine solution for 1 h to inactivate any unreacted GA. These MPs were collected by filtration, washed with ddH_2O, and then lyophilized overnight. Finally, dried MPs were sieved to obtain particles of 50–100 μm in diameter and sterilized with ethylene oxide for 16 h.

2.3. Rabbit MSC isolation and pre-culture

Rabbit MSCs were isolated from the femur of 4-week-old rabbits as previously described [17]. Briefly, after anesthesia, rabbit bone marrow was collected into 10 ml syringe containing 5000 U of heparin. The bone marrow was then filtered through a cell strainer (40 μm) and cultured in DMEM-LG supplemented medium containing 10% v/v fetal bovine serum (Gemini, Calabasas, CA), 250 μg fungizone/l, 100 mg ampicillin/l, and 50 mg gentamicin/l (Invitrogen) for 2 weeks. After cells became confluent, they were released from the flasks with 0.05% trypsin-EDTA (Invitrogen) and placed in medium containing 20% FBS and 10% dimethyl sulfoxide (DMSO) and stored in liquid nitrogen prior to use. A pool of rabbit MSCs from six rabbits was used for all studies. For experiments, cryopreserved cells were thawed at 37 °C, seeded in T-75 flasks, and expanded for 14 days of culture in DMEM supplemented medium containing 10% v/v fetal bovine serum (Gemini, Calabasas, CA), 250 μg fungizone/l, 100 mg ampicillin/l, and 50 mg gentamicin/l.

2.4. Microparticle and rabbit MSC encapsulation

Before encapsulation, OPF and gelatin MPs were sterilized with ethylene oxide for 16 h. Then, sterilized MPs were loaded with TGF-β1 by immersing them in aqueous TGF-β1 solution at pH 7.4 and incubating them at 4 °C for 15 h as has previously been established [9]. At this pH, there is an ionic complex of gelatin MPs and TGF-β1 due to the negative charge of the acidic gelatin (IEP of 5.0) and positive charge of TGF-β1 (IEP of 9.5) [18]. TGF-β1-free MPs were also prepared for comparison.

Following this incubation period, isolated MSCs and gelatin MPs were encapsulated in a network of OPF. First, OPF and the crosslinking agent poly(ethylene glycol)-diacrylate (PEG-DA; Nektar Therapeutics, Huntsville, AL) were combined in 300 μl PBS using a 2:1 ratio of OPF to PEG-DA by weight, and mixed with MPs partially swollen in 110 μl of PBS containing 3.6 ng TGF-β1/μl. Equal volumes (46.8 μl) of the thermal radical initiators, 25 mM ammonium persulfate (APS) and 25 mM *N,N,N′,N′*-tetramethylethylenediamine (TEMED) in PBS were then added. After this mixture was vortexed, a 168 μl PBS suspension containing 6.7 million MSCs was added to achieve a cell concentration

of 10 million cells/ml in the final suspension. After gentle mixing, the suspension was quickly injected into Teflon molds (6 mm diameter, 0.5 mm thickness) followed by incubation at 37 °C for 8 min. Final gel constructs were transferred into 12 well tissue culture plates. Each well contained one gel construct and 1.25 ml medium. The medium was changed every 3 days. At days 3, 7, and 14, samples were collected for biochemical assays ($n = 4$), quantitative reverse transcriptase polymer chain reaction ($n = 4$) and histological analysis ($n = 2$). Samples at day 0 were collected immediately after encapsulation process and used as a control for all other groups. Cell-free, hydrogels ($n = 3$) were also prepared following the same methods. These cell-free, hydrogels were analyzed with samples to establish any background contribution from the hydrogel to fluorescence and absorbance measurements in the biochemical assays.

To examine the effect of hydrogel formulation, the first study included OPF hydrogels containing embedded MSCs, OPF hydrogels containing embedded MSCs and unloaded MPs, and OPF hydrogels containing embedded MSCs and TGF-β1-loaded MPs. Ten million cells/ml of MSCs were encapsulated in each gel construct since a previous study with bovine chondrocytes showed that OPF hydrogels encapsulating a similar number of bovine chondrocytes (9 million cells/ml) showed significant increases in DNA and GAG production in the presence of the TGF-β1-loaded MPs [7]. The second study for the effect of cell-seeding density on differentiation of MSCs used two seeding densities (10 and 20 million cells/ml). In the third study to examine the effect of TGF-β1 concentration on rabbit MSC function, three different concentrations of TGF-β1 (3, 10, and 16 ng/ml) have been loaded into MPs.

2.5. Biochemical assays for cell proliferation and GAG production

At each time point, samples and cell-free hydrogels were removed from medium, rinsed in 2 ml PBS, homogenized with a pellet grinder (Fisher Scientific) and digested in 500 μl of a proteinase K solution (1 mg proteinase K/ml (Sigma-Aldrich), 10 μg pepstatin A/ml (Sigma-Aldrich), and 185 μg iodoacetamide/ml (Sigma-Aldrich)) in tris-EDTA solution (6.055 mg tris(hydroxymethyl aminomethane)/ml (Sigma-Aldrich), 0.372 mg EDTA/ml (Sigma-Aldrich), pH 7.6 adjusted by HCl) at 60 °C for 16 h. After collection and digestion of all samples and cell-free hydrogels, specimens were subjected to three repetitions of a freeze/thaw/sonication cycle (30 min at −80 °C, 30 min at room temperature, 30 min of sonication) to facilitate the complete extraction of DNA from the cell cytoplasm. DNA and GAG assays were then run in triplicate for each experimental and control groups at each time point.

DNA content was calculated by measuring double-stranded DNA content using the PicoGreen assay (Molecular Probes, Eugene, OR) according to the manufacturer's instructions. The fluorescence of negative, cell-free hydrogels was subtracted from the fluorescence values of experimental groups to account for fluorescence of the material alone.

Similarly, glycosaminoglycan content was also determined using a biochemical assay, the dimethylmethylene blue dye (DMMB) assay (Sigma-Aldrich), as previously described [19]. Upon DMMB binding to GAG, a pink color is produced, allowing for quantification of GAG by measuring absorbance at 520 nm. GAG content in hydrogels was calculated by comparison to a curve generated from standards of known amounts of chondroitin sulfate (Sigma-Aldrich). A microplate reader (BIO-TEK Instrument, Winooski, VT) was utilized for both the absorbance/fluorescence measurements.

2.6. Histology

Histology samples were prepared as previously described [7]. Briefly, samples from each time point were rinsed in 2 ml PBS for 1 h and then fixed in 10% neutral buffered formalin (Sigma-Aldrich). After fixation, these samples were dehydrated by immersion in a series of ethanol solutions (70%, 80%, 85%, 90%, 95%, and 100%) and xylene solutions in ethanol (50% and 100%). Specimens were then embedded in paraffin and cross-sectioned to a thickness of 10 μm using a microtome (Microm, Walldorf, Germany). Sections from all groups were simultaneously stained with Safranin-O. Images were acquired with a light microscope (Eclipse E600; Nikon, Melvile, NY) equipped with a video camera (3CCD Color Video Camera DXC-950P; Sony, Park Ridge, NJ).

2.7. Real-time PCR

Total RNA was extracted from hydrogel composites at each time point via the RNeasy Mini Kit (Qiagen). Briefly, hydrogels were transferred into RNA lysis buffer solution and homogenized by gentle pipetting. The homogenized solution was purified using a Qiagen shredder column and total RNA was extracted with the RNeasy Mini Kit. RNA samples were then reverse-transcribed to cDNA using Oligo dT primers (Promega) and superscript III transcriptase (Invitrogen). The final cDNA were then subjected to real time PCR (ABI Biomed 7300 Real-Time PCR System) to determine the expression of genes for type II collagen genes, aggrecan, and type I collagen. PCR reaction was carried out with specific primers and qPCR MasterMix Plus (Eurogentec) containing dNTPs, HotGoldStar DNA polymerase, $MgCl_2$, Urasil-*N*-Clycosylase, SYBR Green I, and stabilizers as described in the manufacturer's instruction. All gene expressions were normalized to expression of the house-keeping gene, glyceraldehyde-3-phosphatase dehydrogenase (GAPDH) and expressed as the fold ratio as compared with a control groups. For these studies, the control group contained MSCs embedded in OPF with unloaded MPs that were analyzed just after encapsulation (day 0). The sequence of primers for GAPDH, type I collagen, type II collagen, and aggrecan were as follows: GAPDH: 5-TCACCATCTTCCAGGAGCGA-3, 5-CACAATGCCGAAGTGGTCGT-3; type I collagen gene: 5-CTTCTGGCCCTGCTGGAAAGGATG-3, 5-CCCGGATACAGGTTTCGCCAGTAG-3; type II collagen gene: 5′-AACACTGCCAACGTCCAGAT-3′, 5′-CTGCAGCACGGTATAGGTGA-3′; Aggrecan: 5′-GCTACGGAGACAAGGATGAGTTC-3′, 5′-CGTAAAAGACCTCACCCTCCAT-3′.

2.8. Statistical analysis

DNA, GAG, and gene expression are reported as means ± standard deviation with $n = 4$. Repetitive ANOVA and Tukey's multiple comparison test were used to determine possible significant differences ($p < 0.05$) in the DNA contents, GAG contents, and gene expression for each group.

3. Results

The composition of each group compared in the study is provided in Table 1. All the rabbit MSCs were homogenously dispersed throughout hydrogels and observed to be intact and viable when encapsulated in OPF hydrogel composites (Fig. 1). The cells were also shown to aggregate around gelatin MPs at later time points (Fig. 1B); cell aggregation was not observed in groups containing only OPF.

3.1. Effect of carrier composition and TGF-β1 release on chondrogenic differentiation of encapsulated MSCs

3.1.1. Biochemical assays

DNA content at each time point is provided in Fig. 2. A significant decrease in DNA content was observed during the first 3 days. However, the DNA content remained statistically unchanged for days 3–14 for all sample types.

GAG content for each composite is shown in Fig. 3. A significant increase in GAG/DNA content was found at days 7 and 14 only in the groups containing gelatin MPs as compared with day 0 controls.

Table 1
Experimental groups of hydrogel composites

	OPF (g)	PEG-DA (g)	Microparticles (g)	TGF-β1 (ng/ml)	MSCs (million cells/ml)
Study 1: effect of formulation of hydrogel composites on MSC differentiation					
Formulation					
OPF	0.1	0.05	—	—	10
OPF + UP	0.1	0.05	0.0219	—	10
OPF + LP	0.1	0.05	0.0219	10	10
Study 2: effect of MSC seeding density of hydrogel composites on MSC differentiation					
Seeding density					
Low cell density	0.1	0.05	0.0219	10	10
High cell density	0.1	0.05	0.0219	10	20
Study 3: effect of TGF-β1 concentration of hydrogel composites on MSC differentiation					
Concentration					
Low dose	0.1	0.05	0.0219	3.6	10
Middle dose	0.1	0.05	0.0219	10	10
High dose	0.1	0.05	0.0219	16	10

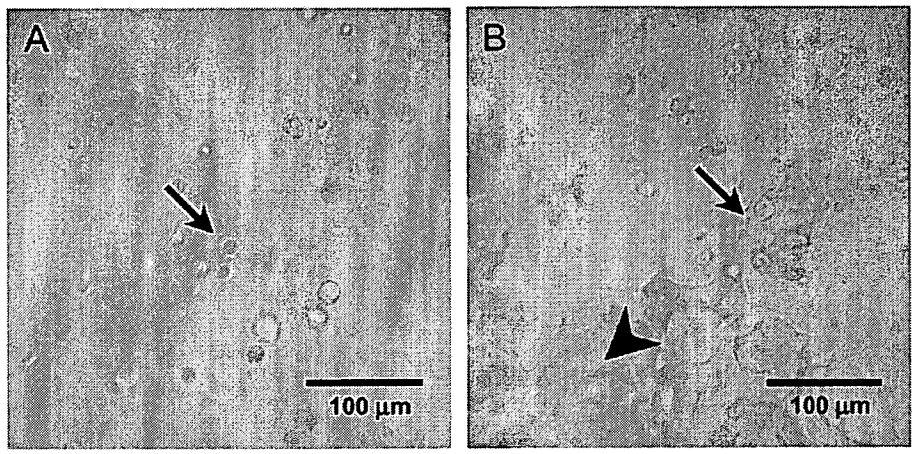

Fig. 1. Light microscopy of OPF hydrogel composites containing rabbit MSCs. Small arrows indicate encapsulated rabbit MSCs, and big arrows indicate encapsulated microparticles. (A) and (B) represent OPF hydrogel composites with only rabbit MSCs and with rabbit MSCs and TGF-β1-loaded microparticles at day 7, respectively.

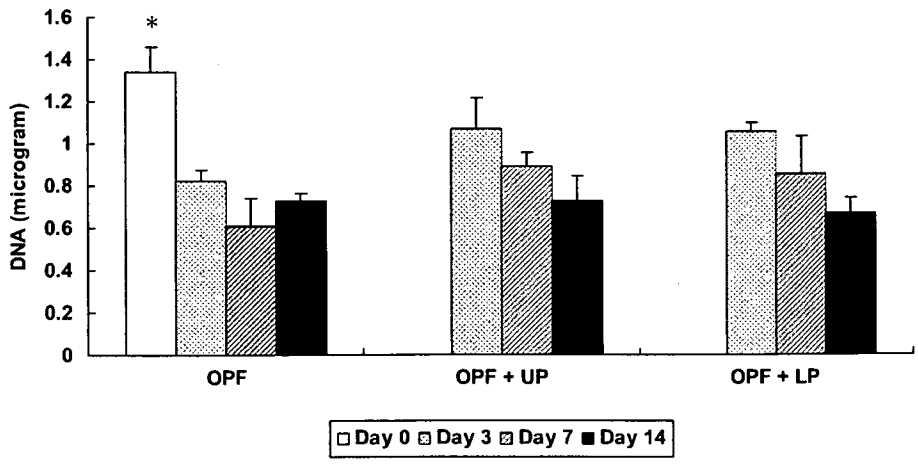

Fig. 2. DNA content of OPF hydrogel composites encapsulating rabbit MSCs, rabbit MSCs and unloaded microparticles, or rabbit MSCs and TGF-β1-loaded microparticles. Samples marked by (*) exhibited significantly higher DNA content than all other groups ($p<0.05$). Error bars represent means ± standard deviation with $n = 4$.

3.2. Histology

The GAG within cell-containing constructs was analyzed by Safranin-O. Fig. 4 displays cross sections of these constructs at days 0 and 14. MSCs (indicated by small arrows) and gelatin MPs (indicated by large arrows) were clearly stained with a deep red color. Due to the different swelling properties of the OPF network and gelatin MPs, the preparation of samples for histology resulted in tearing of some samples. As seen in Fig. 4, cells were homogenously distributed throughout hydrogel composites and, additionally, MSCs maintained a round shape and formed cell aggregates during culture period. Apparently larger cell aggregates were observed in sections of hydrogels with MPs compared to cells in OPF hydrogel without MPs. In addition, a light red background was seen around cell aggregates.

3.3. Real-time PCR

Groups containing TGF-β1-loaded MPs showed a significant increase in collagen type II at day 14 as compared to the control group (no growth factor at day 0), while cells encapsulated in OPF hydrogels without MPs and with MPs without TGF-β1 did not demonstrate an increase in collagen type II gene expression (Fig. 5A).

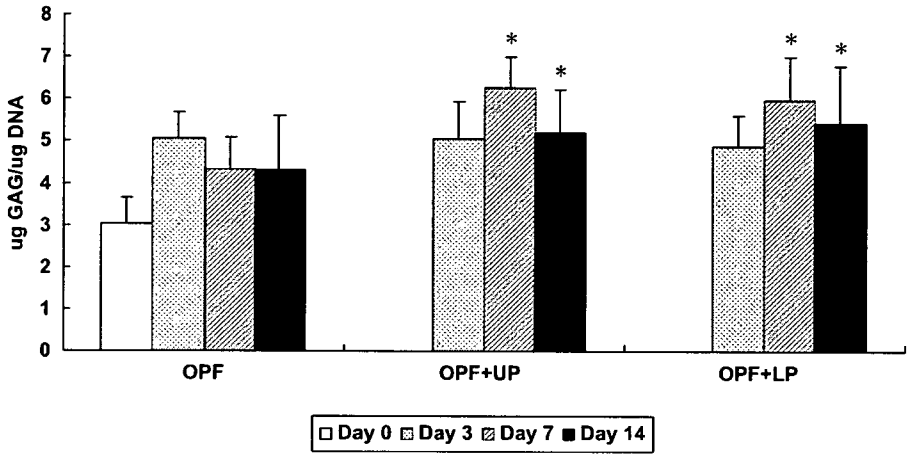

Fig. 3. GAG/DNA content for OPF hydrogel composites encapsulating rabbit MSCs, rabbit MSCs and unloaded microparticles, or rabbit MSCs and TGF-β1-loaded microparticles. Significantly higher ($p<0.05$) GAG/DNA content than day 0 values (controls) are noted with (#). Error bars represent means $\pm$ standard deviation with $n = 4$.

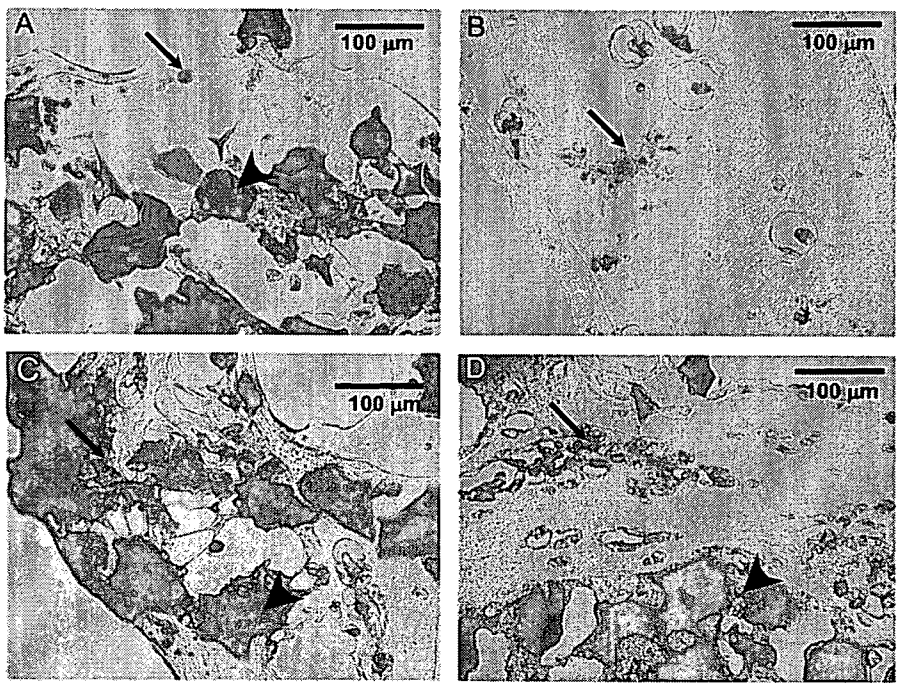

Fig. 4. Cross-sections of OPF hydrogel composites encapsulating rabbit MSCs and TGF-β1-loaded microparticles (A) at day 0. (B)–(D) represent OPF hydrogel composites encapsulating rabbit MSCs, rabbit MSCs and unloaded microparticles, and rabbit MSCs and TGF-β1-loaded microparticles at days 14, respectively. Sections were stained with Safranin-O. A scale bar represents 100 μm for all images.

Aggrecan gene expression was more evident in groups with TGF-β1-loaded MPs. Aggrecan expression showed 93-fold increase compared with controls at day 7 and increased up to 152-fold by day 14 (Fig. 5B). The expression of collagen type I was not significantly different across the culture period (Fig. 5C).

3.4. Effect of cell seeding density in hydrogel composites on chondrogenic differentiation of encapsulated MSCs

3.4.1. Biochemical assays

Although the use of a higher seeding density (20 million cells/ml) resulted in a higher DNA content than those

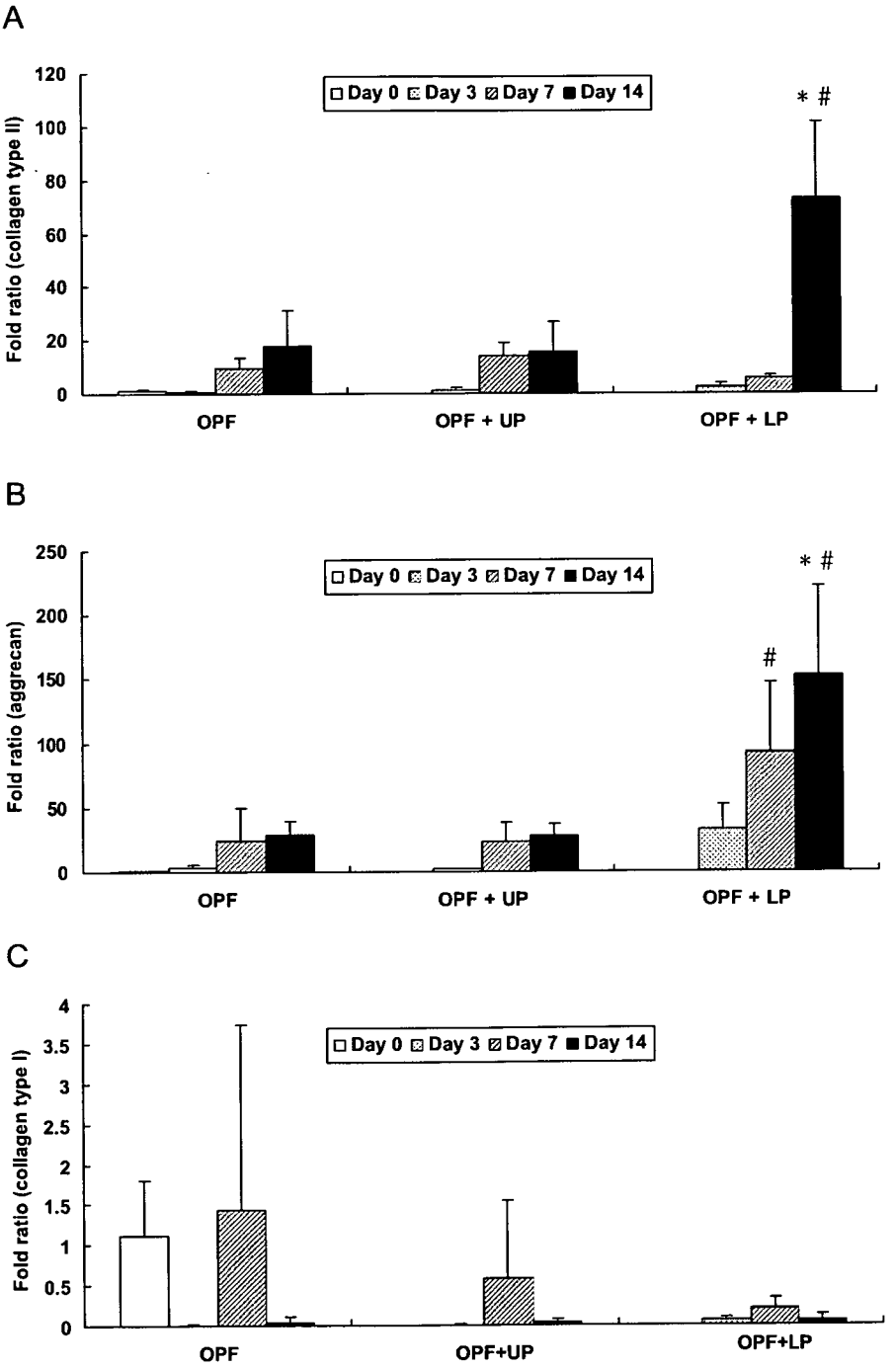

Fig. 5. Quantitative analysis of gene expression for OPF hydrogel composites encapsulating rabbit MSCs (OPF), rabbit MSCs and unloaded microparticles (OPF + UP), or rabbit MSCs and TGF-β1-loaded microparticles (OPF + LP): (A) collagen type II; (B) aggrecan; (C) collagen type I. Data are presented as a fold ratio after normalized to GAPDH. The expression level of controls (day 0) is represented as one. Within a given hydrogel formulation, significantly higher ($p < 0.05$) gene expression than day 0 values (controls) are noted with (#). Samples indicated with (*) had significantly higher gene expression than the other two groups at the same time point ($p < 0.05$). Error bars represent means ± standard deviation with $n = 4$.

measured for the lower seeding density (10 million cells/ml), no significant differences in DNA and GAG/DNA were observed in both groups over the culture period (data not shown).

3.5. Real-time PCR

At 2 weeks, hydrogel constructs with low seeding density showed a 70-fold increase of collagen type II gene expression over controls prepared without growth factor at day 0 while those with high seeding density showed a 30-fold increase (Fig. 6A). At days 7 and 14, only the low seeding density group had aggrecan gene expression that was significantly higher than control groups prepared without growth factor at day 0 (Fig. 6B). Additionally, aggrecan expression was significantly lower in the high seeding density group (a 152-fold increase) as compared with the low seeding density group (a 14-fold increase) at

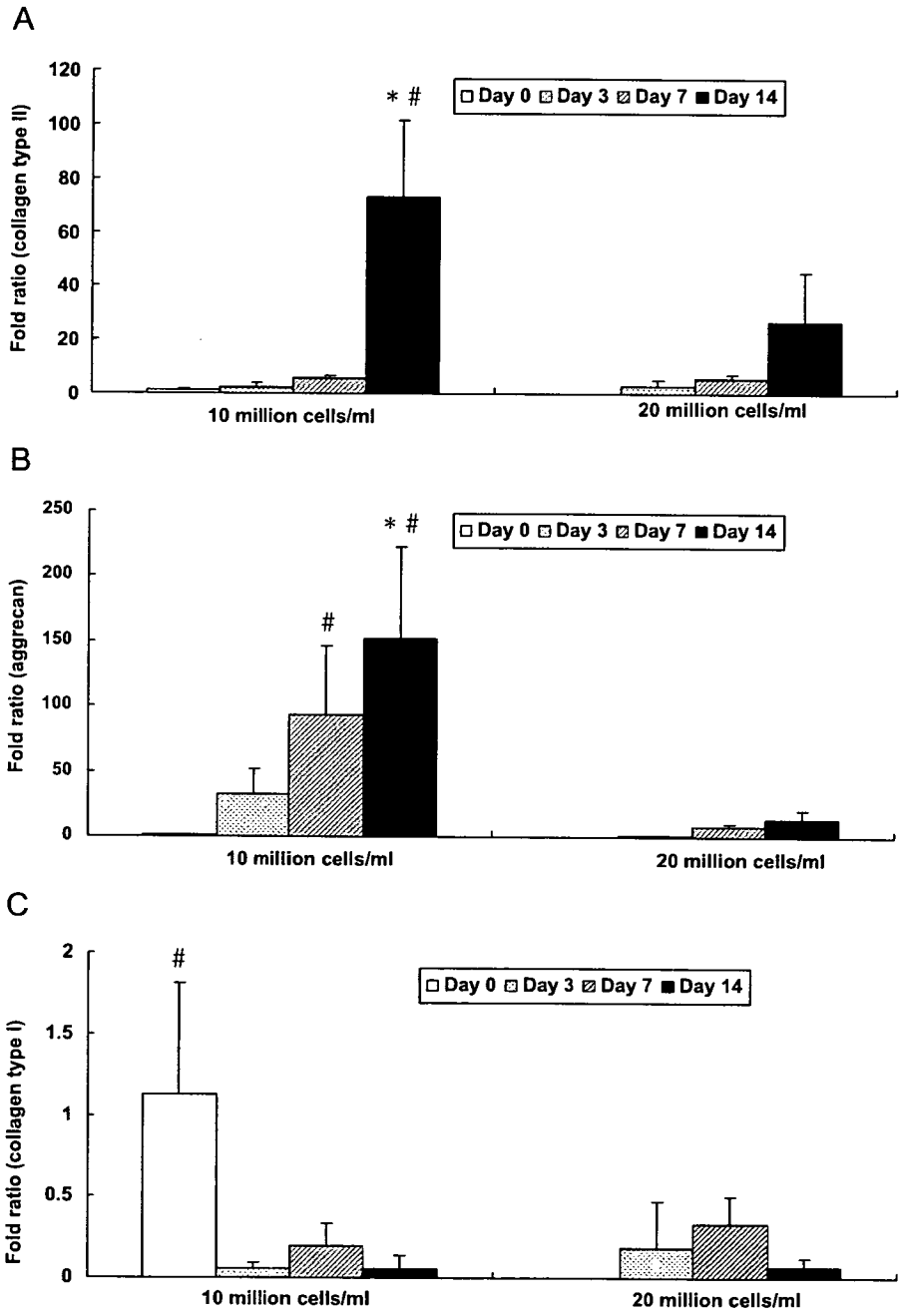

Fig. 6. Quantitative analysis of gene expression for OPF hydrogel composites encapsulating rabbit MSCs and TGF-β1-loaded microparticles with different seeding densities (10 and 20 million cells/ml): (A) collagen type II; (B) aggrecan; (C) collagen type I. Data are presented as fold ratio after normalized to GAPDH. The expression level of controls (day 0) is represented as one. Within a given hydrogel formulation, significantly higher ($p < 0.05$) gene expression than day 0 values (controls) are noted with (#). Samples indicated with (*) had significantly higher gene expression than the other two groups at the same time point ($p < 0.05$). Error bars represent means ± standard deviation with $n = 4$.

day 14. Collagen type I gene expression was downregulated in all groups at day 3 and remained unchanged over culture period, as compared with controls (Fig. 6C).

3.6. Effect of TGF-β1 loading concentration on chondrogenic differentiation of encapsulated MSCs

3.6.1. Biochemical assays

No significant differences in DNA and GAG/DNA were observed in all of the groups over the culture period (data not shown).

3.7. Real-time PCR

Experiments with different concentrations of TGF-β1 revealed that the expression of collagen type II was TGF-β1 concentration-dependent. Cells in high concentration (16 ng/ml) showed the greatest increase over the culture period, resulting in significantly higher expression as compared with low levels (3 and 10 ng/ml) (Fig. 7A). Aggrecan gene expression was also upregulated in concentration-dependent manner. The high concentration group (16 ng/ml) demonstrated a 200-fold increase at day 14, while the medium (10 ng/ml) and low (3 ng/ml) doses showed a 150- and 100-fold increase, respectively (Fig. 7B). As shown in Fig. 7C, type I collagen expression significantly decreased at day 3 than day 0 for all sample types and remained constant at that level during the culture period.

4. Discussion

The objective of this study was to examine the effects of the presence of gelatin microspheres alone or microspheres loaded with TGF-β1 on the chondrogenic differentiation of rabbit MSCs embedded in OPF hydrogels. Additionally, cell proliferation, gene expression and matrix production from encapsulated MSCs were monitored at two cell seeding densities (10 and 20 million cells/ml) and three doses of TGF-β1 (3, 10 and 16 ng/ml) over 14 days *in vitro*.

Due to the scope of this study, three separate experiments were devised (see Table 1). The first, designed to assess the effects of the presence of gelatin MPs and the sustained release of TGF-β1 (10 ng/ml) on chondrogenic differentiation, included the following sample types: rabbit MSCs encapsulated in OPF, rabbit MSCs and MPs without TGF-β1 encapsulated in OPF, and rabbit MSCs and TGF-β1-loaded MPs in OPF.

Results of the DNA assay showed no significant differences in all groups during 14 days of *in vitro* culture except the first 3 days, suggesting that cell death may have occurred during the encapsulation process even though previous studies with OPF hydrogels showed that this system is cytocompatible [7,14]. A similar decrease of DNA was reported with rat calvarial osteoblasts embedded in PEG-DA and rat MSCs encapsulated in OPF hydrogels [14,20]. However, in a study with OPF hydrogels encapsulating bovine chondrocytes, a significant increase in DNA content was found in groups containing gelatin MPs [7], indicating that rabbit MSCs experienced different cellular activity as compared with bovine chondrocytes under the same conditions.

GAG, matrix molecules associated with the chondrocytic phenotype, was measured to examine the chondrogenic differentiation of rabbit MSCs. As shown in Fig. 3, hydrogels containing gelatin MPs showed a significant increase in GAG/DNA content starting at day 7, indicating that gelatin MPs may promote more GAG production compared to hydrogels without gelatin MPs. A previous study with OPF hydrogel encapsulating chondrocytes and gelatin MPs showed a significant increase in GAG production as compared with OPF hydrogels alone [7]. Additionally, it has been reported that rabbit MSCs embedded in PLGA scaffolds modified with gelatin and chondroitin sulfate also showed the increase in GAG production as compared to PLGA alone [21]. However, it appears that MSCs encapsulated in OPF hydrogel composites produced less GAG than when cultured on scaffolds with pore sizes of 500 μm [21]. It is possible that GAG production was limited by the polymer mesh surrounding MSCs.

Histology results showed that rabbit MSCs exhibited a round morphology similar to chondrocytes in hydrogel constructs and also formed cell aggregates in hydrogel composites, indicating that cells were intact, moved together, and interacted with each other throughout the constructs. It is well known that cell condensation occurs in joint development *in vivo*, leading to the formation of cartilage tissue [22]. Therefore, cell–cell contact may be important in promoting chondrogenic differentiation of MSCs in this system.

Additionally, the relative gene expression of collagen type II, aggrecan, and collagen type I was analyzed as an indicator for chondrogenic differentiation of rabbit MSCs with real-time PCR. Production of collagen type II and aggrecan are markers of chondrogenic differentiation of MSCs, while collagen type I produced by fibroblasts or undifferentiated MSCs [23]. The results showed a significant increase in collagen type II expression at day 14 and aggrecan expression starting at day 7 in groups containing TGF-β1-loaded MPs over control groups, indicating that TGF-β1-loaded microparticles promote chondrogenic differentiation of rabbit MSCs. Although GAG/DNA production was increased with the presence of gelatin MPs alone, these results suggest that the presence of TGF-β1 is required to induce expression of chondrocyte-associated genes.

Collagen type I gene expression was consistently low over the culture period, regardless of sample type. A possible explanation for this is that MSCs encapsulated in hydrogels maintained a round morphology during the culture period. In these experiments, the change in shape from a spread morphology during pre-culture to a round morphology after encapsulation could have induced the

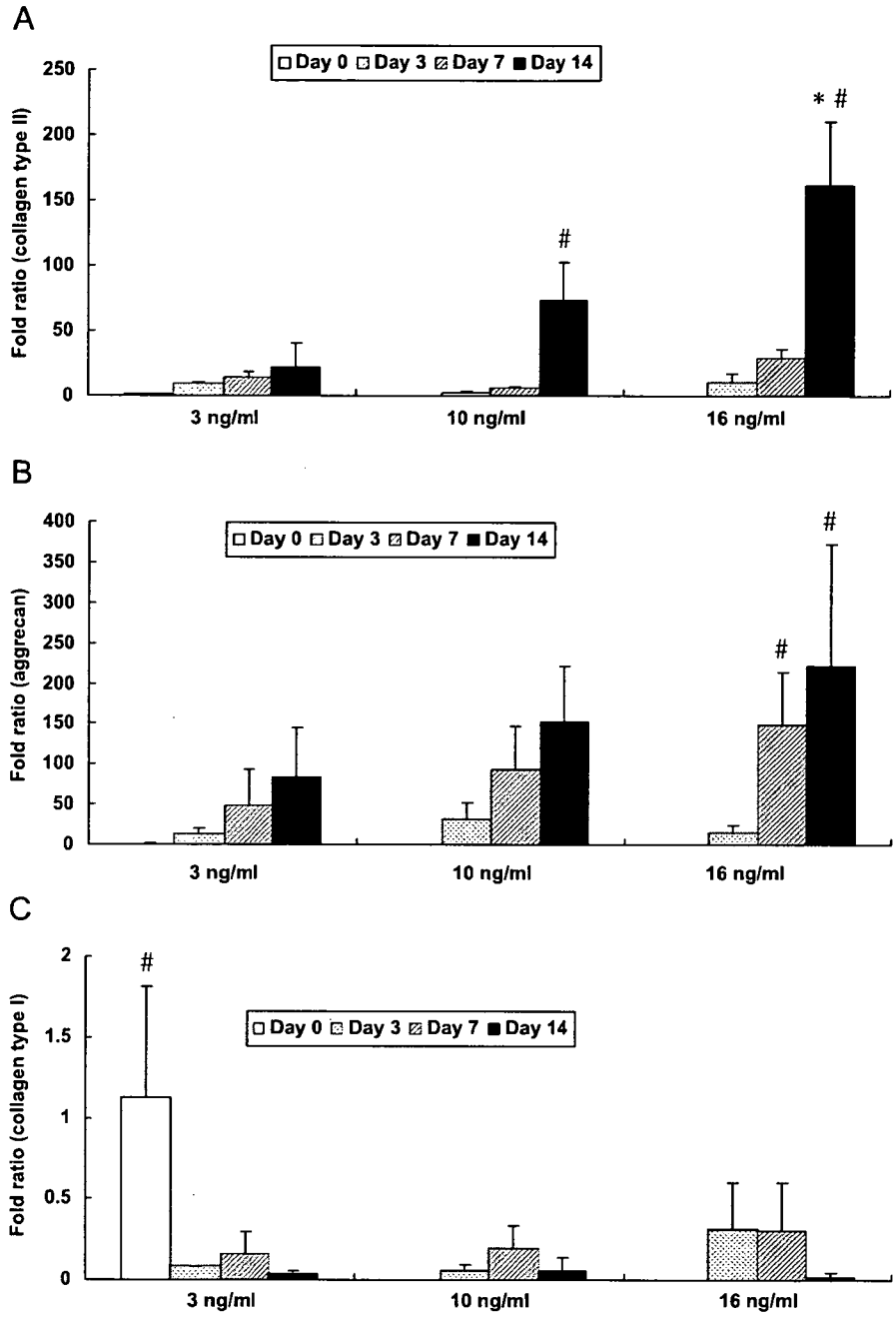

Fig. 7. Quantitative analysis of gene expression for OPF hydrogel composites encapsulating rabbit MSCs and TGF-β1-loaded microparticles with different concentrations of TGF-β1 (3, 10, and 16 ng/ml): (A) collagen type II; (B) aggrecan; (C) collagen type I. Data are presented as fold ratio after normalized to GAPDH. The expression level of controls (day 0) is represented as one. Within a given hydrogel formulation, significantly higher ($p<0.05$) gene expression than day 0 values (controls) are noted with (#). Samples indicated with (*) had significantly higher gene expression than the other two groups at the same time point ($p<0.05$). Error bars represent means $\pm$ standard deviation with $n=4$.

decrease in collagen I expression seen in the first 3 days (and maintained over the remaining culture period). A study with chondrocytes embedded in alginate also showed a similar trend of decreasing collagen type I expression [24].

The effect of seeding density on cell differentiation was also investigated since the cell density is a critical factor for chondrogenic differentiation of MSCs embedded in a scaffold [25]. A previous study with bovine chondrocytes embedded in agarose hydrogels revealed that higher seeding densities (20 and 60 million cells/ml) showed more collagen and GAG content and better mechanical strength over a lower seeding density (10 million cells/ml). However, this study also showed that the highest seeding density (60 million cells/ml) may cause a limitation of nutrient availability [26].

Based on this study, as well as our previous work with bovine chondrocytes seeded at 9 million cells/ml [7], for these experiments we selected two different seeding densities (10 and 20 million cells/ml). Real-time PCR revealed that OPF hydrogel constructs with a low seeding density demonstrated higher collagen type II and aggrecan gene expression at day 14 than those with higher seeding density. Although it has been reported that high cell seeding density promoted more GAG and collagen production by chondrocytes [26], it appears that the chondrocytic gene expression in OPF hydrogel composites was affected more by the TGF-β1 dose than by the seeding density. In this system, because the MPs in both groups were loaded with the same amount of TGF-β1 (10 ng/ml) and the same amount of MPs were applied per gel, the concentration of TGF-β1 that each cell experienced in high density groups could have been relatively lower as compared with low density groups. To further explore this explanation of these results, we examined the effect of TGF-β1 concentration on the chondrogenic gene expression of MSCs embedded in hydrogel constructs in a third set of experiments.

In the third study, three different concentrations of TGF-β1 (3, 10 and 16 ng/ml) in OPF hydrogel composites were used. A pellet culture study with rabbit MSCs showed that lowering the TGF-β1 concentration in the medium decreased chondrogenesis. When rabbit MSC pellets were exposed to 0.5 and 1 ng/ml TGF-β1, they demonstrated partial chondrogenesis in the outer layer of pellets. However, chondrogenesis was observed throughout pellets cultured with 10 ng/ml TGF-β1 [27]. Based on this, 10 ng/ml TGF-β1 was chosen as the "medium dose" for our study. A previous study in our laboratory showed that gelatin MPs loaded with TGF-β1 at 3 ng/ml were able to promote cell proliferation and GAG production when encapsulated in OPF hydrogels with bovine chondrocytes. Thus, 3 ng/ml was selected as the lowest dose. Sixteen ng/ml of TGF-β1 was chosen because a prior experiment revealed that, at this loading concentration, that 10 ng/ml of TGF-β1 was expected to remain in the hydrogel composites at day 14 [7]. The level of gene expression corresponded to the concentration of TGF-β1 initially loaded into the gelatin MPs. Higher gene expression of collagen type II and aggrecan was found in groups with the highest dose of TGF-β1 (16 ng/ml). However, changes in GAG production were not observed, indicating that the upregulation of aggrecan gene expression did not result in an increase in extracellular aggregating species over 14 days. Cells in hydrogel constructs with the lowest dose of TGF-β1 (3 ng/ml) did not show a significant increase over control groups during the culture period, indicating that there may be a threshold dose of TGF-β1 that influence the differentiation of cells in OPF hydrogels. Interestingly, the total amount of TGF-β1 required to have significant effects on chondrogenic differentiation of rabbit MSCs was lower than other *in vitro* studies, suggesting that the localized and sustained delivery of TGF-β1 from gelatin MPs was still able to promote cartilage relevant gene expression of rabbit MSCs. This result indicates that not only does the OPF hydrogel encapsulating gelatin MPs provide a carrier for cells and growth factors, but also functions as an effective way to deliver the growth factor to cells.

5. Conclusion

Rabbit MSCs encapsulated within OPF hydrogel composites remained viable and maintained a round morphology over 14 days *in vitro*. On a per-cell basis, the presence of gelatin MPs promoted GAG production over OPF hydrogels alone. Real-time RT-PCR demonstrated the upregulation of cartilage-relevant genes such as collagen type II and aggrecan when MSCs were encapsulated with MPs loaded with TGF-β1. Additionally, gene expression was dependent on the dose of TGF-β1 originally loaded, suggesting a threshold level of TGF-β1 release is required to induce chondrogenic differentiation in this system, Taken together, these results indicate that OPF hydrogel composites are a promising material for concurrent cell and growth factor delivery for cartilage tissue regeneration.

Acknowledgement

This work has been supported by the National Institutes of Health (R01 AR48756).

References

[1] Temenoff JS, Mikos AG. Review: tissue engineering for regeneration of articular cartilage. Biomaterials 2000;21(5):431–40.
[2] Jackson DWST. Tissue engineering principles in orthopaedic surgery. Clin Orthop 1999;367(Suppl.):31–45.
[3] Kisiday JMJ, Kurz B, Hung H, Semino C, Zhang S, Grodzinsky AJ. Self-assembling peptide hydrogel fosters chondrocyte extracellular matrix production and cell division: implications for cartilage tissue repair. Proc Natl Acad Sci USA 2002;99(15):9996–10001.
[4] Elisseeff JMW, Anseth K, Riley S, Ragan P, Langer R. Photoencapsulation of chondrocytes in poly(ethylene oxide)-based semi-interpenetrating networks. J Biomed Mater Res 2000;51(2):164–71.
[5] Lee KYMD. Hydrogels for tissue engineering. Chem Rev 2001; 101(7):1869–80.
[6] Holland TA, Bodde EW, Baggett LS, Tabata Y, Mikos AG, Jansen JA. Osteochondral repair in the rabbit model utilizing bilayered, degradable oligo(poly(ethylene glycol) fumarate) hydrogel scaffolds. J Biomed Mater Res A 2005;75(1):156–67.
[7] Park H, Temenoff JS, Holland TA, Tabata Y, Mikos AG. Delivery of TGF-beta1 and chondrocytes via injectable, biodegradable hydrogels for cartilage tissue engineering applications. Biomaterials 2005;26(34):7095–103.
[8] Holland TATJ, Tabata Y, Mikos AG. Transforming growth factor-1 release from oligo(poly(ethylene glycol) fumarate) hydrogels in conditions that model the cartilage wound healing environment. J Controlled Rel 2003;94(1):101–14.
[9] Holland TATY, Mikos AG. In vitro release of transforming growth factor-beta 1 from gelatin microparticles encapsulated in biodegradable, injectable oligo(poly(ethylene glycol) fumarate) hydrogels. J Controlled Rel 2003;91(3):299–313.
[10] Jo S, Shin H, Mikos AG. Modification of oligo(poly(ethylene glycol) fumarate) macromer with a GRGD peptide for the preparation of

functionalized polymer networks. Biomacromolecules 2001;2(1): 255–61.
[11] Jo S, Shin H, Shung AK, Fisher JP, Mikos AG. Synthesis and characterization of oligo(poly(ethylene glycol) fumarate) macromer. Macromolecules 2001;34(9):2839–44.
[12] Shin H, Quinten Ruhe P, Mikos AG, Jansen JA. In vivo bone and soft tissue response to injectable, biodegradable oligo(poly(ethylene glycol) fumarate) hydrogels. Biomaterials 2003;24(19):3201–11.
[13] Shin HZK, Farach-Carson MC, Yaszemski MJ, Mikos AG. Modulation of differentiation and mineralization of marrow stromal cells cultured on biomimetic hydrogels modified with Arg–Gly–Asp containing peptides. J Biomed Mater Res 2004;69A(3):535–43.
[14] Temenoff JS, Park H, Jabbari E, Sheffield TL, LeBaron RG, Ambrose CG, et al. In vitro osteogenic differentiation of marrow stromal cells encapsulated in biodegradable hydrogels. J Biomed Mater Res A 2004;70(2):235–44.
[15] Temenoff JS, Park H, Jabbari E, Conway DE, Sheffield TL, Ambrose CG, et al. Thermally cross-linked oligo(poly(ethylene glycol) fumarate) hydrogels support osteogenic differentiation of encapsulated marrow stromal cells in vitro. Biomacromolecules 2004; 5(1):5–10.
[16] Ashcroft GS. Bidirectional regulation of macrophage function by TGF-beta. Microbes Infect 1999;1(15):1275–82.
[17] Solchaga LA, Gao J, Dennis JE, Awadallah A, Lundberg M, Caplan AI, et al. Treatment of osteochondral defects with autologous bone marrow in a hyaluronan-based delivery vehicle. Tissue Eng 2002;8(2): 333–47.
[18] Yamamoto M, Ikada Y, Tabata Y. Controlled release of growth factors based on biodegradation of gelatin hydrogel. J Biomater Sci Polym Ed 2001;12(1):77–88.
[19] Farndale RW, Buttle DJ, Barrett AJ. Improved quantitation and discrimination of sulphated glycosaminoglycans by use of dimethylmethylene blue. Biochim Biophys Acta (BBA)—Gen Subjects 1986;883(2):173.
[20] Burdick JA, Anseth KS. Photoencapsulation of osteoblasts in injectable RGD-modified PEG hydrogels for bone tissue engineering. Biomaterials 2002;23(22):4315–23.
[21] Fan H, Hu Y, Zhang C, Li X, Lv R, Qin L, et al. Cartilage regeneration using mesenchymal stem cells and a PLGA-gelatin/chondroitin/hyaluronate hybrid scaffold. Biomaterials 2006;27(26):4573.
[22] Caplan AI. Review: mesenchymal stem cells: cell-based reconstructive therapy in orthopedics. Tissue Eng 2005;11(7–8):1198–211.
[23] Sobajima S, Shimer AL, Chadderdon RC, Kompel JF, Kim JS, Gilbertson LG, et al. Quantitative analysis of gene expression in a rabbit model of intervertebral disc degeneration by real-time polymerase chain reaction. Spine J 2005;5(1):14–23.
[24] Bonaventure J, Kadhom N, Cohen-Solal L, Ng KH, Bourguignon J, Lasselin C, et al. Reexpression of cartilage-specific genes by dedifferentiated human articular chondrocytes cultured in alginate beads. Exp Cell Res 1994;212(1):97–104.
[25] Kavalkovich KW, Boynton RE, Murphy JM, Barry F. Chondrogenic differentiation of human mesenchymal stem cells within an alginate layer culture system. In Vitro Cell Dev Biol Anim 2002;38(8):457–66.
[26] Mauck RL, Seyhan SL, Ateshian GA, Hung CT. Influence of seeding density and dynamic deformational loading on the developing structure/function relationships of chondrocyte-seeded agarose hydrogels. Ann Biomed Eng 2002;30(8):1046–56.
[27] Johnstone B, Hering TM, Caplan AI, Goldberg VM, Yoo JU. In vitro chondrogenesis of bone marrow-derived mesenchymal progenitor cells. Exp Cell Res 1998;238(1):265–72.

OsteoArthritis and Cartilage (2007) **15**, 187–197

doi:10.1016/j.joca.2006.07.006

Osteoarthritis and Cartilage

International Cartilage Repair Society

OARSI OSTEOARTHRITIS RESEARCH SOCIETY INTERNATIONAL

Degradable hydrogel scaffolds for *in vivo* delivery of single and dual growth factors in cartilage repair

T. A. Holland Ph.D.†, E. W. H. Bodde M.D.‡, V. M. J. I. Cuijpers B.Sc.‡, L. S. Baggett Ph.D.§, Y. Tabata Ph.D.‖, A. G. Mikos Ph.D.†* and J. A. Jansen Ph.D., D.D.S.‡*

† *Department of Bioengineering, Rice University, P.O. Box 1892, MS 142, Houston, TX 77251-1892, USA*

‡ *Department of Periodontology and Biomaterials, Radboud University Nijmegen Medical Center, 309, P.O. Box 9101, 6500 HB Nijmegen, The Netherlands*

§ *Department of Statistics, Rice University, P.O. Box 1892, MS 138, Houston, TX 77251-1892, USA*

‖ *Department of Biomaterials, Field of Tissue Engineering, Institute for Frontier Medical Sciences, Kyoto University, 53 Kawara-cho Shogoin, Sakyo-ku, Kyoto 606-8507, Japan*

Summary

Objective: As our population ages, treatment for joint pain associated with articular cartilage damage is becoming a prevalent challenge. Accordingly, this work investigates local delivery of two regulatory proteins – transforming growth factor-β1 (TGF-β1) and insulin-like growth factor-1 (IGF-1) – to cartilage defects from degradable scaffolds as a potential strategy for improving cartilage repair.

Method: The effects of TGF-β1 and/or IGF-1 delivery on osteochondral repair in adult rabbits were examined through histomorphometric analysis of 11 markers of osteochondral repair.

Results: Complete scaffold degradation occurred allowing for assessment of the healing response at 12 weeks post-surgery. When compared to untreated defects, higher scores were observed with IGF-1-treated defects for the six markers of neo-surface repair: neo-surface morphology, cartilage thickness, surface regularity, chondrocyte clustering, and the chondrocyte/glycosaminoglycan content of the neo-surface and the cartilage surrounding the defect. Surprisingly, the benefits of IGF-1 delivery were not maintained when this growth factor (GF) was co-delivered with TGF-β1, despite numerous *in vitro* reports of the combinatory actions of these GFs.

Conclusions: While localized delivery of IGF-1 may be a promising repair strategy, further *in vivo* assessment is necessary, since fibrous tissue was commonly observed in the neo-surface of all treatment groups. More importantly, this study highlights the need to rigorously examine GF interactions in the wound healing environment and demonstrates that *in vitro* observations do not directly translate to the *in vivo* setting.

Key words: Dual growth factor delivery, Biodegradable hydrogel scaffolds, Cartilage engineering, Rabbit osteochondral defects.

Abbreviations: AC articular cartilage, CC-PBS collagenase-containing PBS, ECM extracellular matrix, IGF-1 insulin-like growth factor-1, GAGs glycosaminoglycans, GF growth factor, MPs microparticles, OPF oligo(poly(ethylene glycol) fumarate), PBS phosphate buffered saline, TGF-β1 transforming growth factor-β1, SD standard deviation.

Introduction

The prevalence of joint pain among adults is projected to steadily increase throughout the next 25 years. In fact, by 2030, an estimated 65 million adult Americans will be diagnosed with arthritis[1]. Accordingly, clinicians, biologists, and biomedical engineers are working to develop new cartilage repair strategies by investigating how various bioactive factors participate in the regulation of healthy articular cartilage (AC)[2,3]. Numerous signaling molecules have been isolated from AC[2]. However, research efforts to understand how multiple factors interact have primarily been limited to *in vitro* studies[4–12]. Given the inherent difficulties associated with maintaining *in vitro* cultured chondrocytes in their differentiated state[13], *in vivo* methods for studying growth factor (GF) interactions in the wound healing environment are necessary.

While a few carriers have been developed for dual GF delivery to calcified and vascular tissues[14–16], cartilage research has yet to employ synthetic carriers for controlled dual drug delivery *in vivo*. Fibrin clots have been utilized for GF localization in chondral defects[17], but in order to investigate how the kinetics of release affect healing, synthetic carriers which allow for precise tailoring of drug release rates and material properties are desired. Toward this goal, our laboratory has developed a novel class of hydrogels to deliver multiple GFs[18,19]. These systems are based on oligo(poly(ethylene glycol) fumarate) (OPF), a water soluble polymer that can be crosslinked to form biodegradable and biocompatible hydrogels[18]. Gelatin microparticles (MPs), incorporated into these gels at the time of crosslinking, have been shown to act as enzymatically digestible porogens to speed *in vitro* scaffold degradation[20].

*Address correspondence and reprint requests to: Dr John A. Jansen, Ph.D., D.D.S., Department of Periodontology and Biomaterials, Radboud University Nijmegen Medical Center, 309, University of Nijmegen, P.O. Box 9101, 6500 HB Nijmegen, The Netherlands. Tel: 31-24-361-4920; Fax: 31-24-361-4657; E-mail: j.jansen@dent.umcn.nl

Received 19 December 2005; revision accepted 23 July 2006.

Sustained GF delivery has been achieved by first loading MPs with the desired GF(s) and then encapsulating these MPs within the OPF network[19,20]. Alternatively, GFs can be entrapped within the OPF phase of composites for accelerated release[19].

Co-encapsulation of bovine chondrocytes with GF-loaded MPs in these gels has demonstrated the stimulatory action of incorporated transforming growth factor-β1 (TGF-β1). In particular, OPF scaffolds co-encapsulating TGF-β1-loaded MPs and bovine chondrocytes were seen to have statistically higher cellularity than constructs co-encapsulating chondrocytes and blank MPs after 21 and 28 days of *in vitro* culture[21]. Most recently, OPF scaffolds were seen to undergo biocompatible degradation and support healthy tissue in-growth in osteochondral defects in 4-month-old, New Zealand White rabbits[18].

The present work employs these OPF scaffolds to investigate the potential roles of TGF-β1 and insulin-like growth factor-1 (IGF-1) in osteochondral repair in adult rabbits, since these GFs are among those most widely investigated for AC repair[2,3]. In particular, TGF-β1, a 25 kDa protein, has been shown to promote the chondrogenic differentiation of progenitor cells[22–24] and to enhance chondrocyte proliferation[21,25,26]. IGF-1, a 7.5 kDa protein, appears to primarily act in an anabolic fashion to increase proteoglycan and type II collagen synthesis[10,27–30]. Accordingly, scaffolds were designed to provide fast, initial release of TGF-β1 as a chemoattractant and morphogen[22,23,31] and/or sustained release of IGF-1 as a stimulator of extracellular matrix (ECM) synthesis[28,29,32,33]. GF loadings were based on concentrations shown to be therapeutic in the treatment of full and partial thickness rabbit and porcine defects[17,34].

To investigate the role of TGF-β1 and IGF-1 in cartilage repair, three different formulations of bilayered OPF hydrogels were fabricated and implanted in rabbit osteochondral defects to spatially localize GF delivery to the approximate region where cartilage is found in a healthy joint. The first two scaffold formulations (Table I) were loaded with either TGF-β1 or IGF-1 to separately examine the effects of these factors on cartilage repair. A third group of scaffolds was loaded with both TGF-β1 and IGF-1 to examine the combinatory role of these molecules. After 12 weeks, tissue repair in untreated defects and in defects treated by scaffold implantation was examined by histomorphometric analysis. Additionally, to estimate GF release from these scaffolds, a 28-day *in vitro* release study was conducted.

Methods

GELATIN MP LOADING

Using established methods, MPs (50–100 μm) were fabricated from gelatin (Nitta Gelatin Inc., Osaka, Japan), crosslinked in 40 mM glutaraldehyde (Sigma, St. Louis, MO), and sterilized by ethylene oxide exposure[18,35]. Sterile MPs were then loaded with IGF-1 (R&D Systems, Minneapolis, MN) by swelling in an aqueous solution of IGF-1 (1.19 μg IGF-1/ml phosphate buffered saline (PBS)) to achieve an overall GF loading of approximately 200 ng IGF-1/g gel in the top crosslinked, layer of scaffolds[19]. Blank MPs were loaded with PBS.

Table I
In vivo *study design*

Scaffold	GF loading (ng/g gel)		Repetitions
	TGF-β1	IGF-1	
TGF-β1	200	0	11
IGF-1	0	200	10
TGF-β1&IGF-1	200	200	11
No scaffold	–	–	11

OPF SYNTHESIS

High molecular weight poly(ethylene glycol) (PEG) (Polysciences, Warrington, PA) with a number average molecular weight (M_n) of 25,400 ± 500 and a weight average molecular weight (M_w) of 41,900 ± 300, was utilized to synthesize OPF (M_n = 32,500 ± 1400, M_w = 74,900 ± 10,000) according to previous methods[35]. The molecular weights of the parent PEG and resulting OPF were determined by gel permeation chromatography (n = 3)[20]. OPF was sterilized by exposure to UV light for 3 h following an established technique[18].

SCAFFOLD FABRICATION

All implanted scaffolds consisted of two layers: a top, cartilage forming layer and a bottom, bone forming layer with respective thicknesses of 1 and 2 mm. These dimensions were chosen as a means of restricting GF loading to the upper portion of defects, rather than as a model of exact anatomy. No GFs or MPs were added to the bone forming layer. This basic scaffold design was modeled after a design previously shown to undergo degradation in a timeframe sufficient to support osteochondral tissue repair[18].

Approximately 4 h prior to implantation, scaffolds were fabricated using a 2 step procedure[18]. To form the bottom layer, 0.15 g OPF was dissolved in 395 μl of PBS containing 14 mg *N,N'*-methylene bisacrylamide (Sigma) as a crosslinking agent. Then, 118 μl PBS, 51 μl of 0.3 M tetramethylethylenediamine (in PBS) (Sigma) and 51 μl of 0.3 M ammonium persulfate (in PBS) (Sigma) were added to initiate crosslinking. After vortexing, the suspension was injected into a cylindrical Teflon mold to a height of 2 mm and incubated at 37°C for 5 min to achieve partial crosslinking, enabling lamination to a second layer[18,35].

During this time, the polymer solution for the top scaffold layer was prepared as outlined above, except that 32 mg IGF-1-loaded or PBS-loaded MPs were added. For scaffolds loaded with TGF-β1, the PBS addition contained 1.65 ng TGF-β1/μl (R&D Systems). The final mixture was injected into the mold to form the upper scaffold layer and incubated at 37°C for 10 min for complete crosslinking.

All PBS, initiator, and bisacrylamide solutions were sterilized prior to use by filtration according to an established procedure[18]. The cytocompatibility of this initiating system has been demonstrated by successful cellular encapsulation of bovine chondrocytes[21] in OPF hydrogels during crosslinking. The final dimensions of all scaffolds matched the dimensions of rabbit osteochondral defects (3 mm in diameter × 3 mm in depth)[36] with the top, scaffold layer containing 200 ng of the indicated GF(s) per g crosslinked gel (Table I).

QUANTIFICATION OF *IN VITRO* GF RELEASE

To approximate the expected *in vivo* release profiles of TGF-β1 and IGF-1, dual release of these GFs from scaffolds was assessed *in vitro* in standard PBS or PBS containing 370 ng bacterial collagenase 1A (Sigma) per ml. Since gelatin is degraded primarily by enzymatic hydrolysis, this collagenase concentration was chosen to model tissue

collagenase concentrations in the synovial fluid of patients with osteoarthritis[37]. Single layer scaffolds (3 mm in diameter and 1 mm in thickness) were crosslinked as described above with the exception that one of the two GF solutions contained a trace amount of I^{125} labeled-GF (Perkin Elmer Life Sciences, Boston, MA) to detect drug release. Thus, two sets of scaffolds were fabricated to separately detect TGF-β1 and IGF-1 release. Previously, GF release from these scaffolds has been shown to be controlled by scaffold composition, rather than protein interactions[19]. Accordingly, the individual release of TGF-β1 and IGF-1 from scaffolds incorporating only one GF was not assessed.

After crosslinking, scaffolds ($n = 6$) were placed in the indicated buffer (3 ml) and were agitated on a shaker table (70 rpm) at 37°C. The supernatant of each specimen was collected and replaced by fresh buffer following an established schedule[19,20]. GF release was determined by correlation of measured radioactivity (Cobra II Autogamma, Packard, Meridian, CT) to a standard curve.

ANIMAL SURGERY

Twenty-four, 6-month-old New Zealand White rabbits were utilized in this study. Adult rabbits were utilized since the capacity for AC repair decreases with age[38]. All surgical procedures were based on an established bilateral, rabbit, osteochondral defect model[18,36] and were approved by the Animal Care and Use Committees of Radboud University Nijmegen and Rice University. This animal model was selected for its ease in animal housing (facility cost and size) while enabling defects to be placed at a biomechanically loaded joint site (medial femoral condyle). Prior to surgery, anesthesia was induced by an intravenous injection of Hypnorm® (0.32 mg/ml fentanyl citrate and 10 mg/ml fluanisone) and atropine. General anesthesia was then maintained by a mixture of nitrous oxide, isoflurane, and oxygen administered through a ventilator. To minimize peri-operative infection risk and post-operative discomfort, antibiotic prophylaxis (Baytril 2.5%, Enrofloxacin 5–10 mg/kg) and Fynadyne® was preoperatively administered.

Following anesthesia, rabbits were immobilized on their back. Both legs were then shaved and disinfected with povodine–iodine. The left knee was exposed through a medial parapatellar longitudinal incision. After lateral luxation of the patella, the medial femoral condyle was exposed. With the knee maximally flexed, a full-thickness defect (3 mm in diameter × 3 mm in depth) was created in the center of the condyle using a dental drill (KAVO, Intrasept 905, KAVO Nederland BV, Vianen, The Netherlands). A 2 mm drill bit was first used to establish a 2 mm diameter defect and then gradually enlarged using drill bits with diameters of 2.8 and 3.0 mm. All bits were fashioned with stop to ensure a defect depth of precisely 3 mm. Debris was removed from the defect with a curette, and the edge cleaned with a scalpel blade.

For rabbits belonging to one of the three experimental groups, an appropriate scaffold was then placed into the defect, while untreated defects remained empty. Subsequently, the patella was repositioned, and the capsule and muscle closed with a continuous 4–0 Vicryl suture. Finally, the skin was closed with single intracutaneous 4–0 Vicryl sutures. This procedure was repeated for the right knee but with this knee receiving a different treatment from that of the left knee. Thus, each treatment group utilized 12 rabbits ($n = 12$). To minimize discomfort, Fynadyne® was administered for 2 days postoperatively. The animals were housed in conventional rabbit cages, which allowed for unrestricted weight-bearing activity, and were observed for signs of pain, infection, and proper activity.

TISSUE PROCESSING

At 12 weeks post-surgery, rabbits were euthanized by intravenous administration of Nembutal (pentobarbital). The tissue surrounding the medial femoral condyle was retrieved en bloc, fixed in 10% buffered formalin (pH 7.4) for 1 week, decalcified in 5% formic acid for 14 days, dehydrated through graded ethanols, and embedded in paraffin. Using a microtome (Leica RM 2265, Leica Microsystems, Bannockburn, IL), longitudinal sections of 6 μm in thickness were taken from the defects' center and lateral and medial edges and then stained with Safranin O to identify the glycosaminoglycans (GAGs) of AC with shades of red and light green as a neutral counter stain.

HISTOMORPHOMETRIC ANALYSIS

Histological sections ($n = 3$) were blindly and independently scored by two evaluators (TH and VJ) using a previously established graded system[18]. This histological scoring method was based on the original O'Driscoll system[39] and examines the extent of neo-tissue in-growth and implant degradation, as well as detailed evaluations of the subchondral and chondral regions (Table II). It should be noted that the scale for thickness of the neo-formed cartilage was modified from its original form[18]. Previously, neocartilage thickness was scored from 0 to 3, with scores of 3 and 2, respectively, indicating cartilage of "increased thickness" and "similar thickness" to normal AC. However, for the present study, this scale was revised so that maximum scores represent the desired healing response for all parameters. Additionally, the criterion for classifying chondral tissue morphology was further specified to clearly distinguish between fibrocartilage and fibrous tissue. In particular, a neo-surface was designated as "fibrous" if less than 75% of its cell population was observed to have a spherical, chondrocyte-like morphology (Table II).

STATISTICAL ANALYSIS

A significance level of 0.05 was utilized for all statistical analysis. The *F* test was used for the comparisons of *in vitro* TGF-β1 and IGF-1 release values. Following previous methods, ordered logistic regression of histological scores was performed using SAS Version 8.2 statistical software (SAS, Cary, NC, USA) to analyze the potential single factor effects of treatment group and location within the defect (edge vs center sections)[18,40]. Figures display average values ± standard deviation (SD) of the measured variable.

Results

IN VITRO GF RELEASE

TGF-β1 and IGF-1 release experiments estimated GF release kinetics from OPF scaffolds (Fig. 1) in standard PBS and in collagenase-containing PBS (CC-PBS). The later buffer was utilized since gelatin MPs degrade primarily by enzymatic hydrolysis[20]. High TGF-β1 burst release occurred within the first 3 days (65.5 ± 3.3% in PBS and 60.8 ± 3.4% in CC-PBS) as expected for proteins released from the OPF phase of scaffolds. More specifically, GFs are released by diffusion as OPF scaffolds swell, and burst

Table II
Histological scoring system for the overall defect (a), subchondral region (b), and chondral region (c)

(a) Overall defect evaluation (throughout the entire defect depth)	Score
1. Percent filling with neo-formed tissue	
100%	3
>50%	2
<50%	1
0%	0
2. Percent degradation of the implant	
100%	3
>50%	2
<50%	1
0%	0
(b) Subchondral bone evaluation	Score
3. Percent filling with neo-formed tissue	
100%	3
>50%	2
<50%	1
0%	0
4. Subchondral bone morphology	
Normal, trabecular bone	4
Trabecular, with some compact bone	3
Compact bone	2
Compact bone and fibrous tissue	1
Only fibrous tissue or no tissue	0
5. Extent of neo-tissue bonding with adjacent bone	
Complete on both edges	3
Complete on one edge	2
Partial on both edges	1
Without continuity on either edge	0
(c) Cartilage evaluation	Score
6. Morphology of neo-formed surface tissue	
Exclusively AC	4
Mainly hyaline cartilage	3
Fibrocartilage (spherical morphology observed with ≥75% of cells)	2
Only fibrous tissue (spherical morphology observed with <75% of cells)	1
No tissue	0
7. Thickness of neo-formed cartilage	
Similar to the surrounding cartilage	3
Greater than surrounding cartilage	2
Less than the surrounding cartilage	1
No cartilage	0
8. Joint surface regularity	
Smooth, intact surface	3
Surface fissures (<25% neo-surface thickness)	2
Deep fissures (25–99% neo-surface thickness)	1
Complete disruption of the neo-surface	0
9. Chondrocyte clustering	
None at all	3
<25% chondrocytes	2
25–100% chondrocytes	1
No chondrocytes present (no cartilage)	0
10. Chondrocyte and GAG content of neo-cartilage	
Normal cellularity with normal Safranin O staining	3
Normal cellularity with moderate Safranin O staining	2
Clearly less cells with poor Safranin O staining	1
Few cells with no or little Safranin O staining or no cartilage	0
11. Chondrocyte and GAG content of adjacent cartilage	
Normal cellularity with normal GAG content	3
Normal cellularity with moderate GAG content	2
Clearly less cells with poor GAG content	1
Few cells with no or little GAGs or no cartilage	0

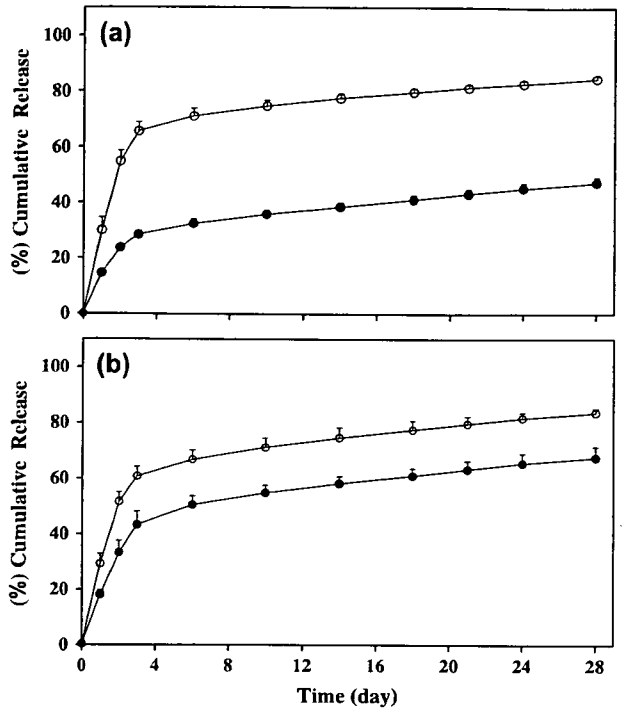

Fig. 1. *In vitro* IGF-1 (●) and TGF-β1 (○) release from OPF scaffolds in PBS (a) and in CC-PBS (b). Data are shown as average cumulative release with error bars representing ±SD ($n = 6$).

release is greatly influenced by hydrogel mesh size[19,35]. Lower burst release was expected for IGF-1 since gelatin MPs were utilized as an intermediate carrier, making drug release dependent on enzymatic degradation of the gelatin network and diffusion through the scaffold[19,20]. Indeed, IGF-1 burst release was only 28.4 ± 1.4% in PBS and 43.3 ± 4.9% in CC-PBS, statistically lower than the corresponding values for TGF-β1 release. Likewise, 28-day cumulative IGF-1 release in PBS (47.3 ± 2.0%) and in CC-PBS (67.4 ± 4.0%) was significantly lower than the corresponding TGF-β1 release values (84.6 ± 1.1% in PBS and 83.6 ± 1.5% in CC-PBS).

ANIMAL HEALTH AND MACROSCOPIC JOINT APPEARANCE AT RECOVERY

Animals regained full movement within approximately 1 week with normal behavior and movement observed throughout the 12-week period. It should be noted that five specimens were removed from the study due to complications common to adult rabbits but unrelated to the surgeries (obstructed digestive tract and pre-existing bacterial skin infection). Accordingly, each treatment group included 10–11 specimens. With these joints, no signs of inflammation, infection, or swelling were noticed upon visible inspection of the joint surfaces at 12 weeks.

HISTOLOGICAL APPEARANCE

Three histological sections per defect were observed by light microscopy, allowing for assessment of the healing response at the defect edges and center (Figs. 2, 4–7). The subchondral regions of untreated defects contained a majority of osseous tissue. However, in eight of 11 defects, cartilaginous tissue regions occupied up to 30% of the

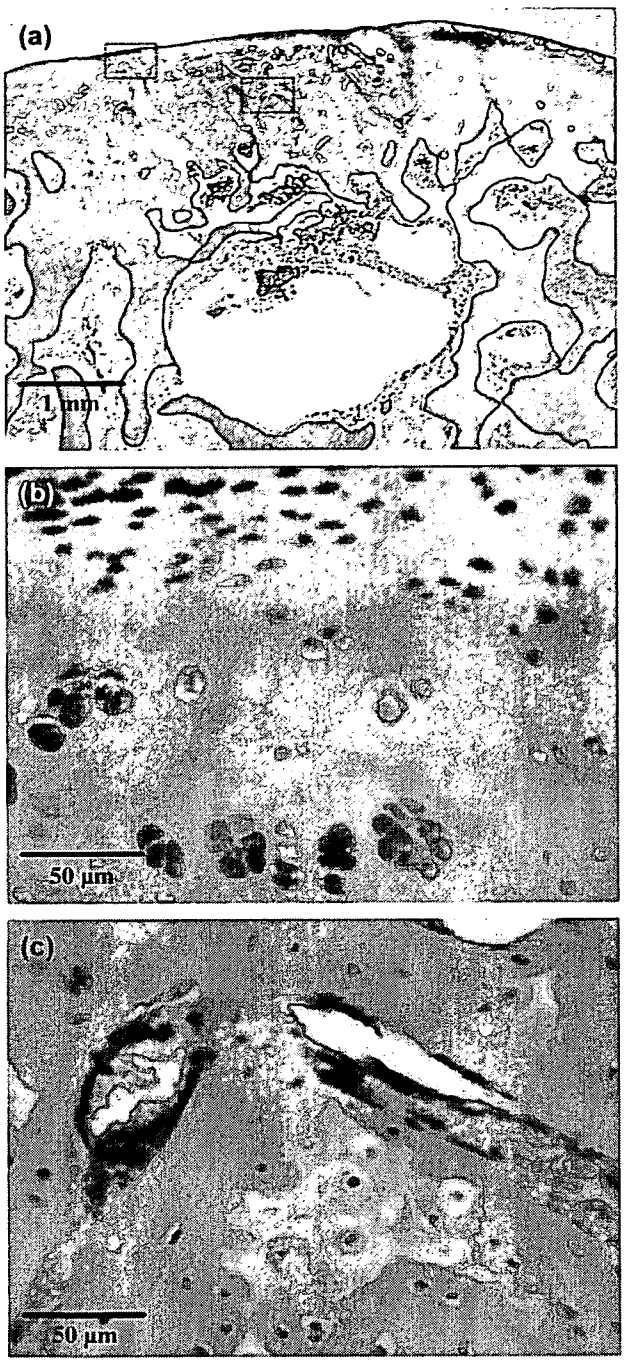

Fig. 2. Histological section displaying fibrocartilage in-growth near the chondral defect margins and significant subchondral restoration. The boxed regions in (a) (2× magnification) are shown at 20× magnification to illustrate the spherical shape of cartilage cells in the neo-surface (b) and small regions of remodeling tissue in subchondral region (c). This defect was treated by IGF-1 delivery.

subchondral region. These regions were generally covered by a fibrous surface and primarily existed at the subchondral/chondral interface. However, in some cases, this un-remodeled tissue penetrated as far as 2 mm from the joint surface. The neo-surface of untreated defects was mainly composed of fibrous tissue and often extended into the joint space (Fig. 4). In general, the neo-surface of control specimens was highly disrupted by fissures.

In all sections of specimens treated with OPF scaffolds, no remaining hydrogel material or MPs were observed, and degradation appeared to be complete at 12 weeks (Figs. 2, 5–7). The subchondral regions of these defects were generally filled with a majority of trabecular bone. However, like untreated defects, regions of hypertrophic cartilage were also visible at the subchondral/chondral interface in some specimens within each treatment group. The frequency of these hyaline subchondral regions (number of defects per treatment) was 45%, 27%, and 18% in TGF-β1-, TGF-β1&IGF-1-, and IGF-1-treated defects, respectively. Figure 5 shows the most striking example of cartilaginous tissue remaining in the subchondral region. However, it should be noted that in all other defects, these regions were confined to less than 30% of the subchondral zone. In fact, complete subchondral restoration with trabecular bone and complete integration with the surrounding osseous tissue were frequently observed (Fig. 7).

The neo-formed surface morphology of defects treated with scaffolds was primarily composed of fibrous tissue of variable thickness, but fibrocartilage was observed in several specimens within each group. Intense Safranin O staining and zonal organization of chondrocytes, indicative of true AC, were rarely observed. However, regions of cartilage-like cells were often visible near the defect margins (Fig. 2), but true AC repair with a zonal organization of cells was only observed in one defect (an IGF-1-treated defect). Very thin fibrous tissue was sometimes observed with all experiment treatments and tended to accompany complete or near complete subchondral restoration, as exemplified by Figs. 2 and 7. In other specimens, thick surface tissue with fissures was observed, especially when subchondral remodeling was incomplete (Fig. 6).

HISTOMORPHOMETRIC ANALYSIS

Quantitative scoring of 11 markers of osteochondral repair (Table II)[18] examined the potential effects of GF delivery and location within the defect (edge vs center). Section location within the former defect did not significantly impact any of the 11 markers of osteochondral repair, indicating that the observed tissue response was generally uniform throughout the defect. However, it should be noted that regions of un-remodeled subchondral tissue were often located toward the middle of the subchondral zone on lateral, medial, and center sections. New bone and chondrocytes appeared to infiltrate the subchondral and chondral regions from the defect margins.

No significant differences in overall tissue filling and implant degradation were observed among the four treatment groups [Fig. 3(a)]. All sections received maximal scores for scaffold degradation, and scores for overall tissue filling approached but did not equal the maximal score. This difference was due to the very thin neo-surface tissue often observed amongst specimens from all treatment groups.

Likewise, average scores for bone filling and bone morphology were below their maximal scores [Fig. 3(b)] since un-remodeled regions were observed in all treatment groups. However, the high average scores for bone integration reflect the complete integration commonly observed with all treatments. Although the frequency of inadequate bone filling was highest amongst untreated defects, scaffold implantation was not observed to significantly influence subchondral bone repair. However, improved bone healing with scaffold implantation was not expected since growth delivery was confined to the upper portion of osteochondral defects, and repeated research has demonstrated that

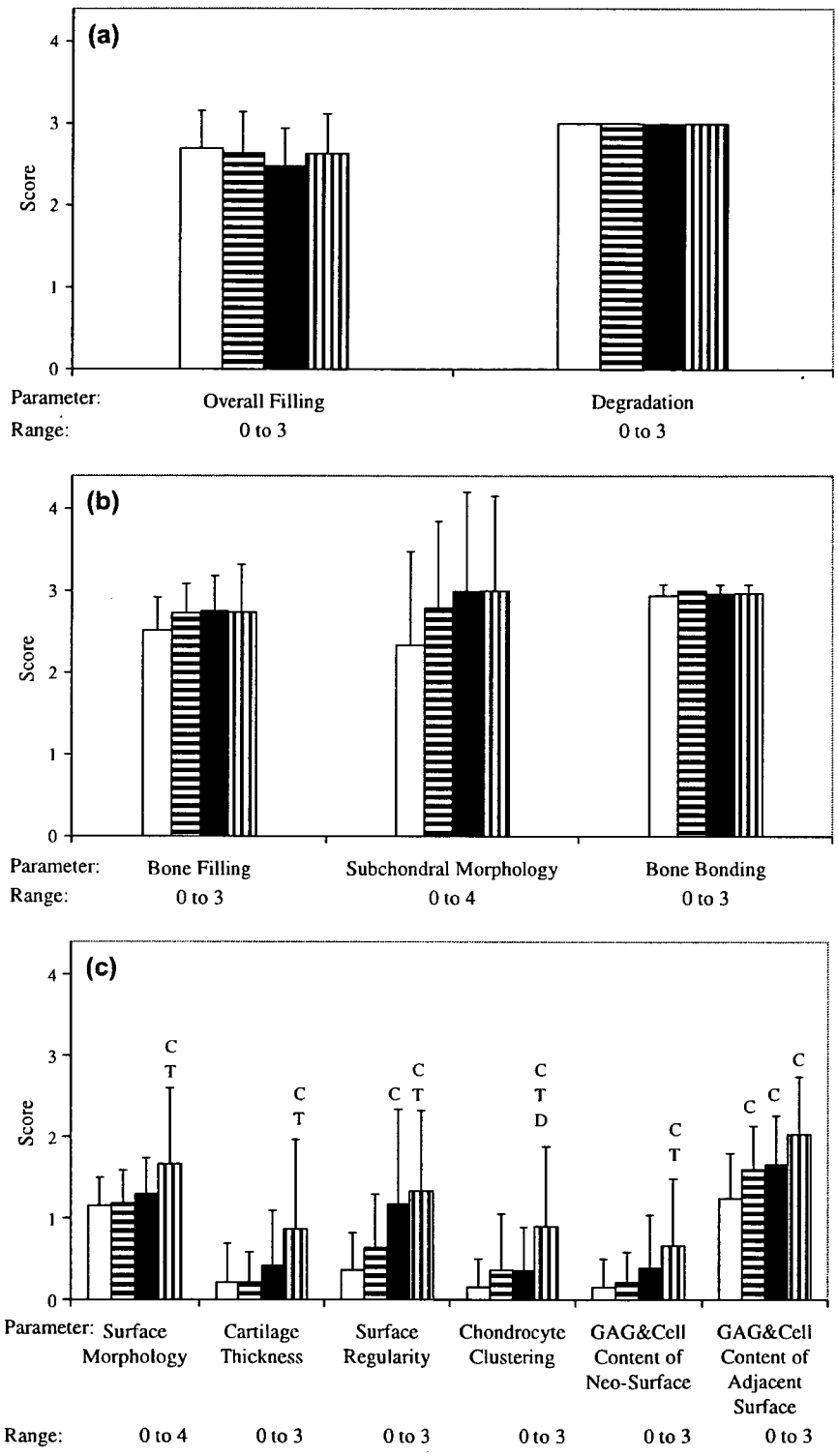

Fig. 3. Comparison of results following histomorphometric analysis of the overall defect (a), subchondral region (b), and chondral region (c). Data are shown as average scores with error bars representing ±SD ($n = 10-11$ defects per treatment). Scores with significant differences ($P < 0.05$) compared to untreated defects (control), defects treated by TGF-β1-loaded scaffolds, and defects treated by dual TGF-β1&IGF-1-loaded scaffolds are, respectively, indicated by C, T, and D. Untreated control, □; TGF-β1-delivery, ▤; TGF-β1&IGF-1 delivery, ■; IGF-1 delivery, ▥.

scaffolds alone often serve as insufficient templates to guide tissue regeneration[41–46]. Since the goal of this study was to examine the GF interactions in cartilage repair, GFs were not delivered to the subchondral bone.

As shown in Fig. 3(c), defects treated by IGF-1 delivery had significantly higher scores for six indicators of neo-surface repair when compared to untreated defects. Additionally, IGF-1 delivery resulted in higher scores for five of the

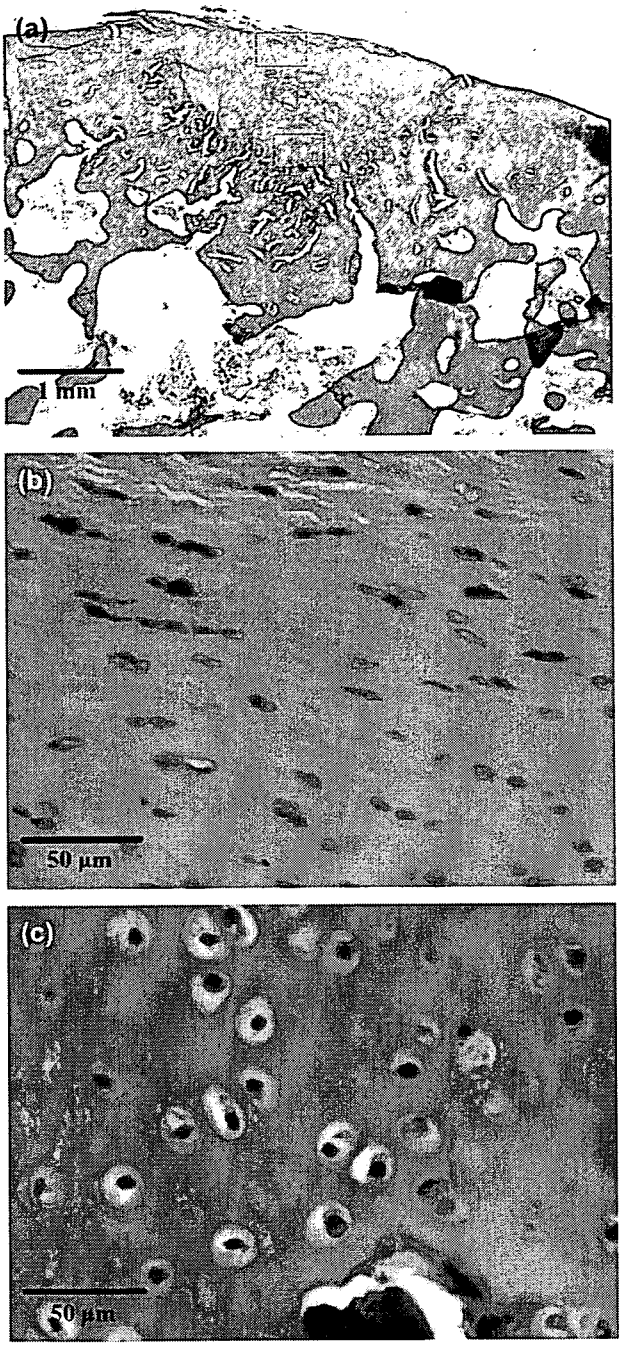

Fig. 4. Histological section displaying the thick fibrous tissue commonly observed at the neo-surface and that often accompanied unremodeled cartilaginous regions in the subchondral zone. The boxed regions in (a) (2× magnification) are shown at 20× magnification to illustrate the cell morphology observed in portions of the chondral (b) and subchondral (c) regions. This defect was untreated.

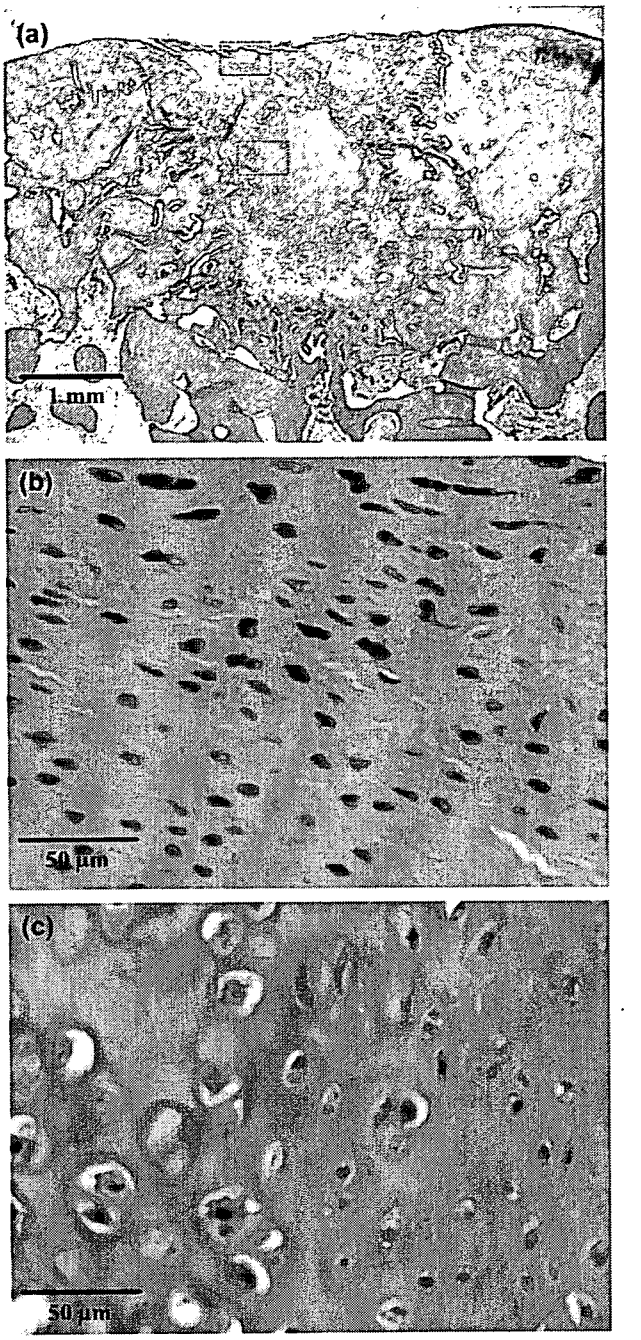

Fig. 5. Histological section displaying the most striking example of cartilaginous tissue remaining in the subchondral defect area. The boxed regions in (a) (2× magnification) are shown at 20× magnification to illustrate the fibrous tissue and hypertrophic cartilage observed in portions of the chondral (b) and subchondral (c) regions, respectively. This defect was treated by IGF-1 delivery.

six markers of neo-surface repair (surface morphology, cartilage thickness, surface regularity, chondrocyte clustering, and the GAG and cell content of the neo-surface) when compared to TGF-β1 delivery. However, when compared to untreated defects, TGF-β1 delivery, as well as TGF-β1&IGF-1 co-delivery, only improved scores for the GAG and cell content of the cartilage surrounding the defect. These results suggest the potential of IGF-1 delivery strategies in chondral repair. However, since a large variation in tissue quality was observed within this treatment group, these findings should be interpreted cautiously. True AC with a zonal arrangement of chondrocytes was only observed in one IGF-1 treated defect, leading to higher average scores and SDs for this treatment group. As reflected by the average scores in Fig. 3(c), fibrous tissue was generally observed in the neo-surface of all treatments.

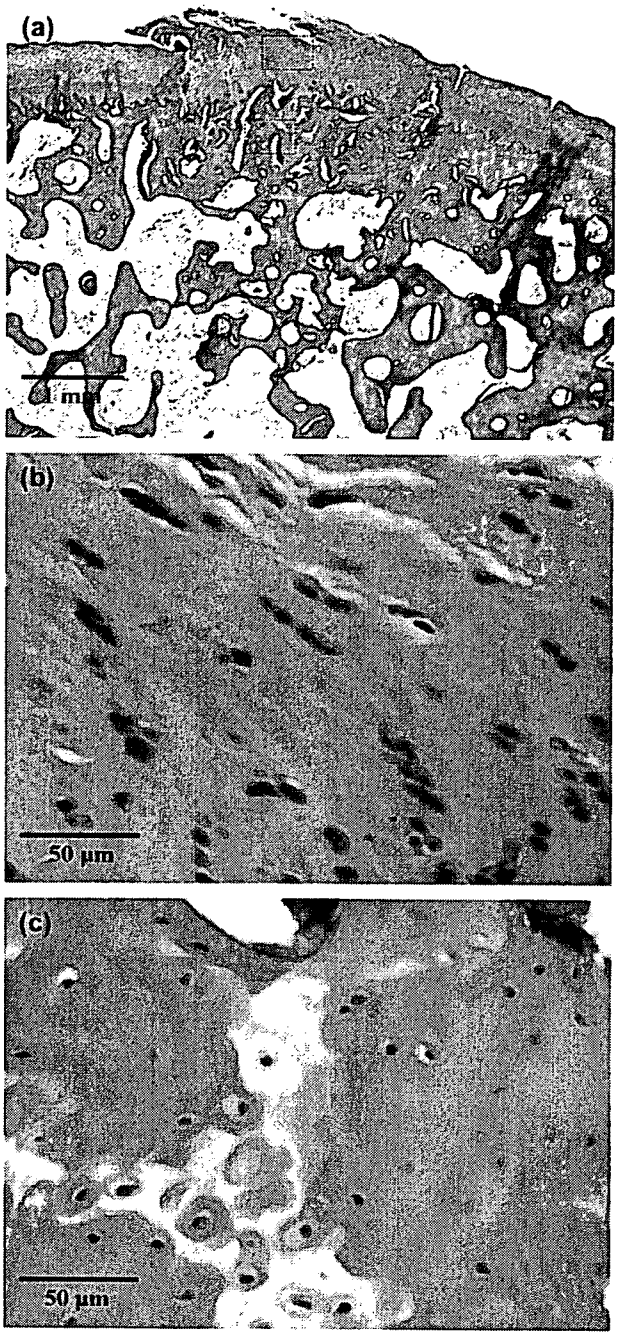

Fig. 6. Histological section displaying excessive fibrous tissue growth into the joint space and significant subchondral restoration. The boxed regions in (a) (2× magnification) are shown at 20× magnification to illustrate the spindle-like cells in the neo-surface (b) and small regions of remodeling tissue in subchondral region (c). This defect was treated by TGF-β1 delivery.

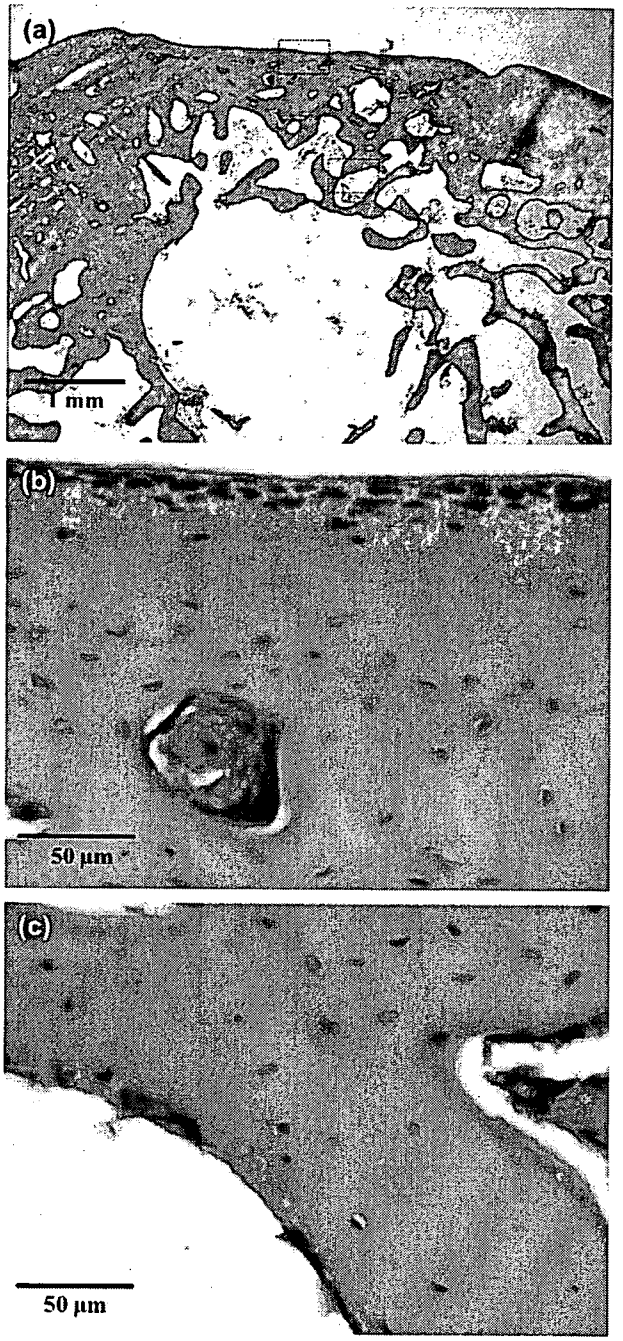

Fig. 7. Histological section displaying thin fibrous tissue growth along the surface of a joint with complete subchondral restoration. The boxed regions in (a) (2× magnification) are shown at 20× magnification to illustrate the morphology of the fibrous neo-surface (b) and the mature bone in the subchondral region (c). This defect was treated by TGF-β1&IGF-1 delivery.

Only 30–40% of IGF-1, TGF-β1, and TGF-β1&IGF-1-treated defects, and 20% of untreated defects, had sufficient "cartilage-like" cells to meet the criterion for the classification as non-fibrous [Table II(c)].

One of the most interesting findings of this study centered upon the apparent lack of TGF-β1 and IGF-1 synergy when simultaneously delivered to osteochondral defects. Compared to untreated defects, treatment with both GFs only improved scores for only two parameters: the regularity of the neo-surface and the chondrocyte/GAG content of the adjacent surface. However, it should again be noted, that these GFs were delivered with different release kinetics. While IGF-1 was expected to be delivered throughout the first several weeks of healing, TGF-β1 was expected to be delivered to the wound site within the first few days.

Discussion

Numerous scaffolds have been investigated for cartilage drug delivery[2], but as of yet, these scaffolds have not been employed to examine the *in vivo* effects of multiple GFs. OPF scaffolds have numerous material parameters which can be manipulated to achieve desired drug release rates[19,20,35] and to study delivery of multiple GFs. Here, we examine *in vivo* delivery of two proteins, TGF-β1 and IGF-1, whose single and combined effects have been the focus of numerous *in vitro* investigations.

TGF-β1 has been shown to promote *in vitro* chondrogenic differentiation of mesenchymal stem cells and chondrocyte proliferation[21–24,47,48]. However, stimulation of GAG synthesis and mRNA expression for type II collagen, important markers of the chondrogenic phenotype, frequently do not accompany TGF-β1-stimulated proliferation[5,12,21]. However, several studies have demonstrated that together TGF-β1 and IGF-1 can synergistically promote proliferation, GAG synthesis, and collagen II expression *in vitro*[6,8,9,12]. These results are not surprising since IGF-1 was initially identified for its ability to promote GAG incorporation into proteoglycans and has been shown to regulate cartilage matrix synthesis[27,28,33]. Due to these reports, scaffolds for *in vivo* analysis of possible TGF-β1/IGF-1 synergy were designed to provide fast, initial release of TGF-β1 (Fig. 1) as a morphogen in the earlier stages of healing[22,23] and sustained release of IGF-1 as a progression factor[28,29,32,33].

Surprisingly, when these scaffolds were used in the repair of osteochondral defects in adult rabbits, combinatory delivery of TGF-β1 and IGF-1 did not result in widespread improvement to the quality of the neo-surface when compared to untreated defects. Dual delivery of TGF-β1 and IGF-1 only appeared to improve neo-surface regularity (vs untreated defects), indicating that findings of *in vitro* TGF-β1 and IGF-1 synergy do not directly correlate with *in vivo* observations. These inconsistencies may be due to the complex *in vivo* environment and the numerous cell types involved in the healing response. For example, previous studies have demonstrated TGF-β1's pluripotent stimulation of chemotaxis and proliferation of inflammatory cells, fibroblasts, chondrocytes, and other cells[31,34,49,50].

The stimulatory activity of TGF-β1 incorporated into OPF hydrogels has previously been demonstrated *in vitro*. Specifically, co-encapsulation of TGF-β1-loaded MPs and bovine chondrocytes within OPF hydrogels was seen to stimulate *in vitro* cell proliferation when compared to chondrocytes co-encapsulated with unloaded MPs[21]. The present study again utilized OPF-gelatin MP networks to deliver TGF-β1 *in vivo*, but TGF-β1 was not seen to improve *in vivo* repair. These findings again suggest the drastically different *in vivo* and *in vitro* environments. However, since the TGF-β1 release kinetics in the present *in vivo* study and aforementioned *in vitro* study were slightly different, results cannot be directly compared. In the present study, approximately 60% of the TGF-β1 was expected to be delivered to the surrounding tissue within 72 h post-surgery, while more sustained release of TGF-β1 was expected in the *in vitro* study.

Furthermore, it should be noted differences in animal models may also give rise to vastly different cellular environments. The TGF-β1 dose utilized in the present study (200 ng/g crosslinked gel) was previously reported to stimulate cell recruitment to porcine and rabbit chondral defects[17,31]. Additionally, a similar TGF-β1 concentration (600 ng/ml) was reported to stimulate partial cartilage repair when utilized in combination with an antiangiogenic factor in full-thickness porcine defects[34]. While these reports were utilized as a starting point for determining GF doses in the current model, differences in the animal species, defect dimension and location (patellar groove vs femoral condyle), and scaffold material properties may lead to vastly different healing situations.

Since high dosages of exogenous TGF-β1[51–54] have frequently been associated with *in vivo* formation of osseous or chondroid outgrowths in joints, increases in the amount of TGF-β1 delivered *in vivo* should be avoided. In the present study, numerous instances of excessive tissue growth at the neo-surface were observed in defects treated by TGF-β1 and TGF-β1&IGF-1 delivery, as well as in untreated defects. Accordingly, IGF-1 may be a more promising candidate than TGF-β1 for delivery strategies, especially since this GF appears to act primarily as a progression factor[33].

Here, individual delivery of IGF-1 resulted in consistently higher scores than untreated defects and defects treated with only TGF-β1 [Fig. 3(c)]. However, given the large variation in healing responses in IGF-1-treated defects, these results do not conclusively confirm the therapeutic ability of this GF. Instead, these results and the apparent lack of TGF-β1&IGF-1 synergy demonstrate the necessity for *in vivo* studies to more accurately examine the role of GFs in healing. This study assessed the effects of rapid TGF-β1 and/or sustained IGF-1 delivery to osteochondral defects. Future work should entail a more detailed examination of the effects of various TGF-β1 and IGF-1 release kinetics upon healing.

Additionally, the present study's thorough histological analysis led to several other interesting observations. Our findings of hyaline cartilaginous regions in the subchondral zone agree with previous reports[55] and the suggestion that the post-injury response involves a rapid influx of mesenchymal cells into the defect area and the fabrication of embryonic-like cartilage tissue throughout the defect (Fig. 5) and sometimes into the joint space[55,56]. As shown in Fig. 4, this cartilage appears to become hypertrophic in the subchondral zone as bone formation is initiated at the defect margins and progressively inward. These observations support previous suggestions that vascularization, resulting in bone formation, controls the rate at which the cartilaginous tissue disappears[56]. However, the cartilage repair tissue near the chondral surface, initially isolated from vascularization, appears to undergo a simultaneous, but separate remodeling as illustrated by the fibrous tissue along the neo-surface in Figs. 4–6. Since spherical chondrocyte-like cells and GAG staining were primarily observed near the chondral defect margins (Fig. 2), cells near the joint surface appear to play a major role in this process[17,31].

Understanding the role of GF interactions in chondrogenesis will undoubtedly prove beneficial, since very thin surface tissue commonly accompanied complete subchondral restoration in this study (Fig. 6) and in other investigations[55,57]. GF delivery via scaffolds remains a logical strategy for AC repair, but this study highlights the need for the caution when interpreting the implications of *in vitro* studies. As evident by this research, the *in vitro* effects of GFs, including the synergistic actions of multiple factors, may not always translate to the wound healing environment. Thus, thorough *in vivo* analysis of GF interactions in tissue repair is necessary. The flexible design properties of OPF hydrogels allow these scaffolds to be used as powerful tools to explore the effectiveness of various GF delivery regimes in the cartilage wound healing environment